materials, for example during the forming process, corresponds to:

$k\Delta T = 0$: adiabatic evolution
$r = 0$: no internal heat production generated by external sources
$(\partial\boldsymbol{\sigma}/\partial T)\dot{\boldsymbol{\varepsilon}}^{e} = 0$, $(\partial A_k/\partial T)\dot{V}_k = 0$: no thermomechanical coupling.

$A_k\dot{V}_k$ represents the nonrecoverable energy stored in the material. For metals, this is the energy of the field of the residual microstresses which accompany the increase in the dislocation density. It represents only 5–10% of the term $\boldsymbol{\sigma}:\dot{\boldsymbol{\varepsilon}}^{p}$ and is often neglible:

$$A_k\dot{V}_k \approx 0.$$

The equation of adiabatic overheating is given by:

- $$\rho C_\varepsilon \dot{T} = \boldsymbol{\sigma}:\dot{\boldsymbol{\varepsilon}}^{p}.$$

Bibliography

Germain P. & Muller P. *Introduction à la mécanique des milieux continus.* Masson, Paris (1980).
Germain P. *Cours de mécanique des milieux continus.* Masson, Paris (1973).
Valid R. *La mécanique des milieux continus et le calcul des structures.* Eyrolles, Paris (1977).
Bamberger Y. *Mécanique de l'ingénieur, II: Milieux déformables.* Hermann (1981).
Nemat-Nasser S. *Mechanics today.* Vol. I, II, III, IV, V. Pergamon Press, New York (1972–1980).
Sanchez-Palencia E. *Non homogeneous media and vibration theory.* Springer Verlag, Berlin (1980).
Truesdell C. *The elements of continuum mechanics.* Springer Verlag, Berlin (1966).
Eringen A. C. *Mechanics of continua.* J. Wiley, New York (1967).
Kestin J. & Rice J. R. *A critical review of thermodynamics.* Stuart Ed. Mono book (1970).

3

IDENTIFICATION AND RHEOLOGICAL CLASSIFICATION OF REAL SOLIDS

L' expérience (d'un Laboratoire), c'est l'ensemble des erreurs qu'on ne recommencera plus.

Continuum mechanics and thermodynamics (Chapter 2) constitute the basic theoretical tools for the formulation of the physical phenomena of deformation and fracture. For fundamental and practical reasons, we model each broad class of phenomena separately. The aim of this chapter is to differentiate from a qualitative point of view and identify the most common types of material behaviour. The phenomenological method used is based on observed experimental results. We, therefore, present some basic elements on the types of tests, the machines and the modern measurement techniques likely to be used. Progress in electronics, automatic controls, digital measurements, and more recently in microprocessors has resulted in a radical transformation, especially during the 1970s, of the laboratories engaged in characterization of materials. We no longer have to be content with approximate measurements of a few quantities; we are now in a position to measure the evolution of any mathematically well defined variable precisely. The identification of complex models has thus become possible, but it requires numerical methods for the identification of nonlinear processes which still belong to the domain of 'heuristic' techniques.

The resulting schematic classification allows us to associate, *a priori*, to each material, a theory of only the dominant phenomena in a limited domain of state variables. Beyond its fundamental interest, this offers a guide for the choice of material in the design stage and helps to simplify the estimation of the resistance of a structure under service loads. The method used is that of rheology initiated by Bingham around 1930, with decisive developments taking place during the 1950s.

3.1 The global phenomenological method

We generally distinguish three broad methods for formulating the constitutive laws of materials.

> The microscopic approach attempts to model the mechanics of deformation and fracture at the atomic, molecular and crystalline levels as described in Chapter 1; the macroscopic behaviour being the result of an integration or of an averaging process performed over the microscopic variables at the scale of the volume element of continuum mechanics.
>
> The thermodynamic approach introduces a homogeneous continuous medium equivalent to the real medium and represents microscopic physical phenomena by means of macroscopic 'internal variables'.
>
> The functional approach leads to the hereditary laws of the integral type which appear as characteristic functions of materials, and which are themselves expressed in terms of macroscopic variables. This approach will be partly used in the section on viscoelasticity in Chapter 4.

None of these three approaches allows direct identification of materials. Microscopic variables (density of dislocation, density of cavities, texture...) are difficult to measure, and moreover are difficult to use in practical computations. Thermodynamic potentials are practically inaccessible to measurement, and internal variables, by definition, cannot be measured directly. As the hereditary functions need the knowledge of the whole history of the observable variables, they pose theoretical as well as experimental problems.

The global phenomenological method consists in studying the volume element of matter through the relations between cause and effect which exist between the physically accessible variables constituting the input and output of the process under study. In this way, we are able to determine the material response to a specific input. These responses are sufficient to characterize the materials qualitatively, but they do not constitute (except for linear phenomena) the constitutive laws.

By a volume element, in the sense of solid mechanics, we mean a volume of a size large enough with respect to the material heterogeneities, and small enough for the partial derivatives of the equations of the continuum to be meaningful. Table 3.1 gives the order of magnitude of the reasonable sizes

Table 3.1. *Orders of magnitude of representative volume elements*

Materials	Inhomogeneities	Volume element
Metals and alloys	Crystals 1 μm–0.1 m	0.5 × 0.5 × 0.5 mm
Polymers	Molecules 10 μm–0.05 mm	1 × 1 × 1 mm
Wood	Fibres 0.1 mm–1 mm	1 × 1 × 1 cm
Concrete	Granulates $\simeq$ 1 cm	10 × 10 × 10 cm

of representative volume elements, below which size it becomes illusive, to give a physical meaning to stress or strain other than as an average over the 'homogenized' volume in question.

The physically accessible variables of the volume element are those that can simply be deduced from the four classical and measurable magnitudes of mechanics: displacement, force, time, temperature.

> The strains and their rates:
> total three-dimensional strain $\boldsymbol{\varepsilon}$, or one-dimensional ε, with its large deformation expression $\varepsilon_v = \ln(1+\varepsilon)$,
> reversible elastic strain $\boldsymbol{\varepsilon}^e$ or ε^e,
> permanent strain $\boldsymbol{\varepsilon}^p$ or ε^p.
> The three-dimensional stress $\boldsymbol{\sigma}$, or one-dimensional stress σ, with the approximate expression for large deformations $\sigma_v \simeq \sigma(1+\varepsilon)$.
> The temperature T.
> The time t or the number of cycles to rupture t_R or N_R.

The classification resulting from the global phenomenological method should not be considered intrinsic. It provides, in fact, only a frame of reference for general characteristics. The behaviour of a given material can be represented by a schematic model only in relation to the envisaged usage and the desired precision of the predictions.

A given piece of steel at room temperature can be considered to be:

> Linear, elastic for structural analysis,
> viscoelastic for problems of vibration damping,
> rigid, perfectly plastic for calculation of the limit loads,
> hardening elastoplastic for an accurate calculation of the permanent deformations,
> elastoviscoplastic for problems of stress relaxation,
> damageable by ductility for calculation of the forming limits,
> damageable by fatigue for calculation of the life-time,
> etc.

3.2 Elements of experimental techniques and identification process

3.2.1 *Characteristic tests*

The classical characteristic tests are essentially conducted in simple tension, or tension–compression at constant temperature. The classification of real solids is therefore based upon these tests. The specimen is subjected to an axial load (force or displacement) which produces a uniform state of stress or strain within the whole useful volume of the specimen which can be considered as one volume element. What follows applies to isotropic materials; some complementary remarks concerning anisotropic materials are given at the end of this section.

The uniaxial state is defined by a one-dimensional state of stress and a two-dimensional state of strain:

$$\sigma = \begin{bmatrix} \sigma & 0 & 0 \\ 0 & 0 & 0 \\ 0 & 0 & 0 \end{bmatrix} \qquad \varepsilon = \begin{bmatrix} \varepsilon & 0 & 0 \\ 0 & -\nu^*\varepsilon & 0 \\ 0 & 0 & -\nu^*\varepsilon \end{bmatrix}$$

where ν^* is the coefficient of contraction, equal to Poisson's ratio ν in elasticity.

In elastoplasticity or elastoviscoplasticity the hypotheses of the decoupling of elastic and plastic strains ($\boldsymbol{\varepsilon} = \boldsymbol{\varepsilon}^e + \boldsymbol{\varepsilon}^p$) and of plastic incompressibility ($\mathrm{Tr}\,(\boldsymbol{\varepsilon}^p) = 0$) allow us to express the contraction coefficient ν^* simply as:

$$\begin{bmatrix} \varepsilon & 0 & 0 \\ 0 & -\nu^*\varepsilon & 0 \\ 0 & 0 & -\nu^*\varepsilon \end{bmatrix} = \begin{bmatrix} \varepsilon_e & 0 & 0 \\ 0 & -\nu\varepsilon_e & 0 \\ 0 & 0 & -\nu\varepsilon_e \end{bmatrix} + \begin{bmatrix} \varepsilon_p & 0 & 0 \\ 0 & -\frac{1}{2}\varepsilon_p & 0 \\ 0 & 0 & -\frac{1}{2}\varepsilon_p \end{bmatrix}$$

$$\nu^* = \nu\frac{\varepsilon_e}{\varepsilon} + \frac{1}{2}\frac{\varepsilon_p}{\varepsilon}$$

or with the help of the linear-elastic law: $\varepsilon_e = \sigma/E$, as:

$$\nu^* = \frac{1}{2} - \frac{\sigma}{E\varepsilon}\left(\frac{1}{2} - \nu\right).$$

The graph of this function, compared with some experimental results for an aluminium alloy with hardening characteristics similar to the curve in Fig. 3.2, is given in Fig. 3.1.

Hardening test in simple tension or compression

This is the most common test. The specimen is subjected to a deformation at constant speed. The response consists of a variation in the stress σ as a function of the strain ε showing the hardening of the material (Fig. 3.2).

Fig. 3.1. Elastoplastic coefficient of contraction for aluminium alloy AU4G (2024).

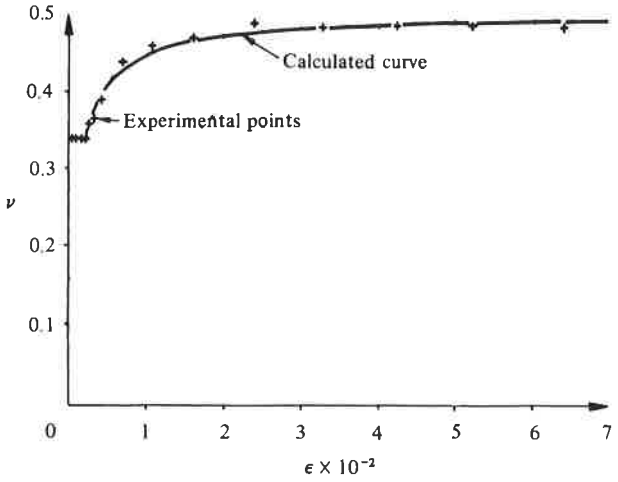

Fig. 3.2. Hardening test.

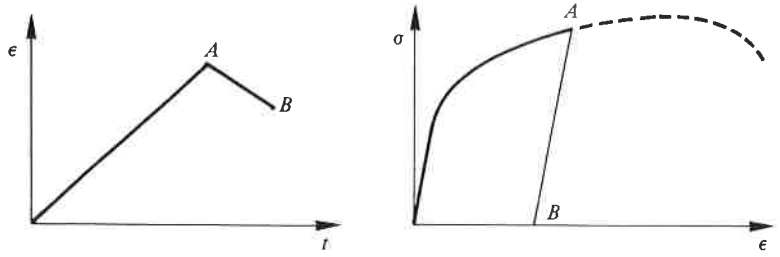

Fig. 3.3. Creep test and subsequent recovery.

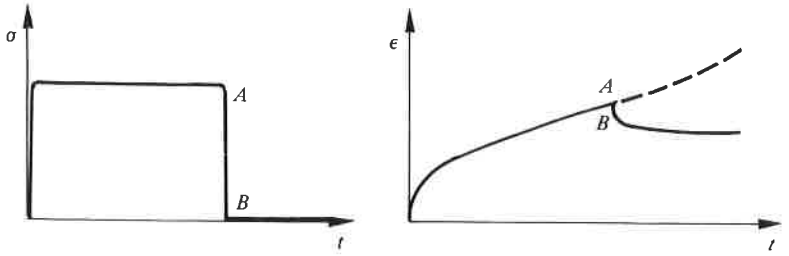

Creep test in simple tension or compression

In this test the specimen is subjected to a constant state of stress (generally apparent stress) and the resulting variation in strain ε as a function of time t is determined. This also characterizes the hardening and the viscosity of the material (Fig. 3.3). The strain variation after the stress is removed (point B) corresponds to the recovery test. The partial strain recovery is indicated on the right hand side of Fig. 3.3.

Relaxation in simple tension or compression

This test is complementary to the preceding one in that the stress response to a constant state of strain is determined. It is governed mainly by the

Fig. 3.4. Relaxation test.

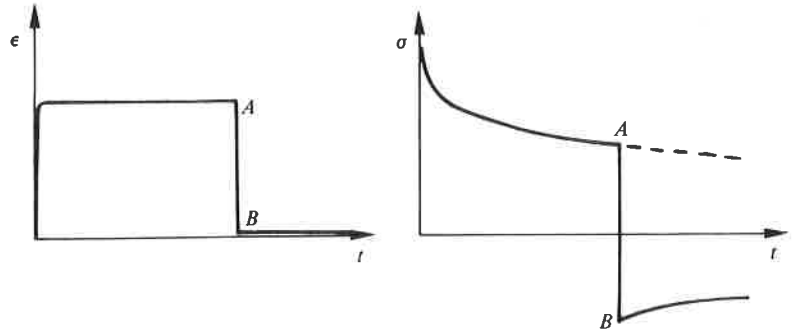

Fig. 3.5. Multiple hardening-relaxation test.

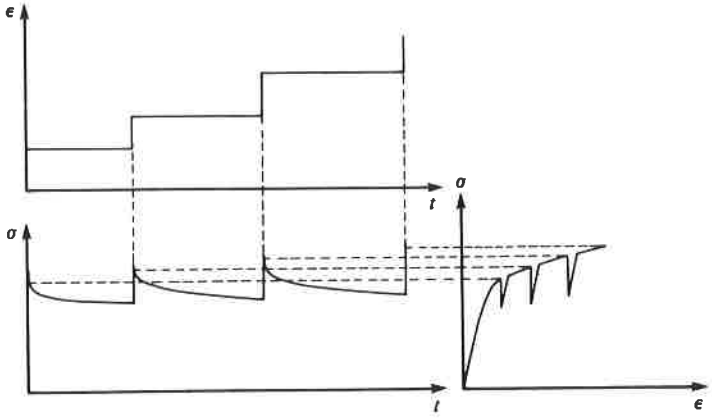

viscosity but also depends on the hardening induced by the initial load (Fig. 3.4).

Multiple hardening-relaxation test

As the name indicates, this test combines the two types of tests and allows us to determine from a single test on a single specimen the hardening characteristics, and also the viscosity, by means of successive relaxations each at different strain levels (Fig. 3.5).

Fig. 3.6. Cyclic test under prescribed strain.

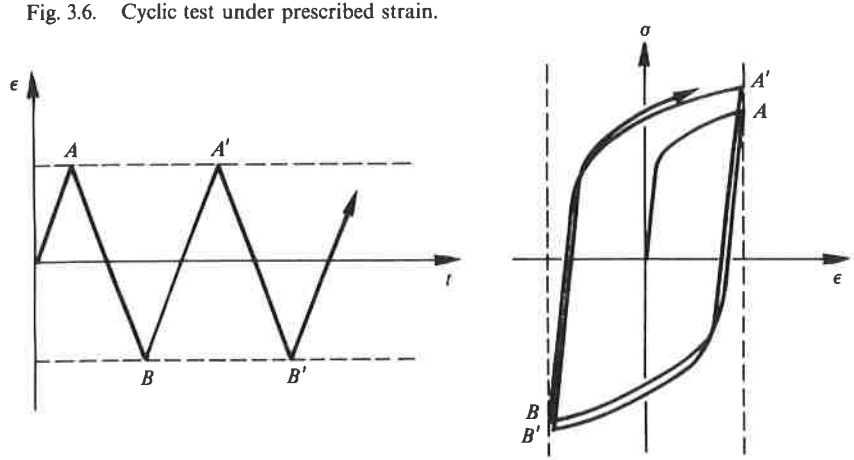

Fig. 3.7. Cyclic hardening curve.

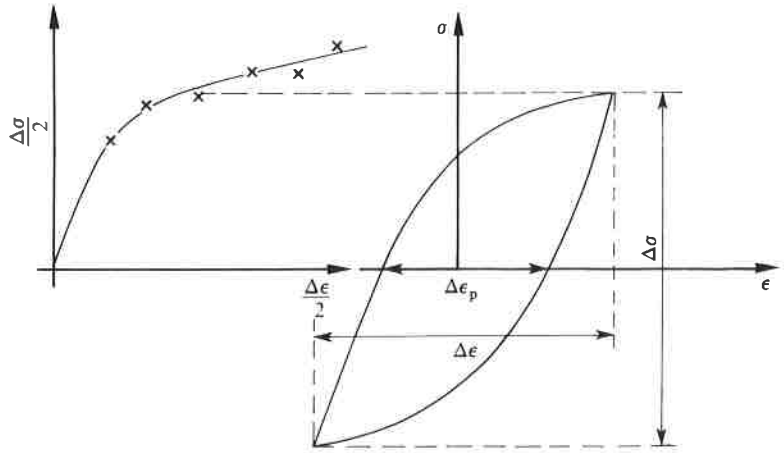

Cyclic test

In this test the specimen is subjected to a periodic load (stress or strain) and the evolution of the cyclic responses is studied by obtaining a (σ, ε) graph (Fig. 3.6). In general the response tends to be stabilized after a certain number of cycles. We can then obtain the cyclic curve which represents a relation between the peaks of the stabilized loops, corresponding to different stress or strain levels (Fig. 3.7). In the case of polymeric materials, or, more generally, in viscoelastic materials the peaks of the loops are difficult to define. We then speak of 'harmonic' tests.

Fracture tests

The four preceding types of tests are also used to determine the corresponding fracture conditions:

stress and strain at fracture;
time or number of cycles to fracture;
energy dissipated in fracture.

Certain characteristics require the use of specimens of a particular geometry (notched specimens for measuring impact strength in the Charpy test, cracked specimens for measuring toughness, etc.).

Multiaxial tests

Unfortunately, these tests are rarely conducted because of the experimental difficulties they present. Among the possible tests are: tension–shear (or compression–shear), biaxial tension and triaxial compression. The tension–shear test performed on circular tubes subjected to tension and torsion is the most interesting one for the characterization of anisotropy. The tension force and the twisting couple are applied either simultaneously or successively and the corresponding rotation and length changes are recorded.

Problems of anisotropic materials

There are even greater difficulties in the case of anisotropic materials, that is when preferred directions exist in the material.

The tension or compression test is still easy to interpret when done along a principal direction of anisotropy.

The torsion test on hollow specimens is more tricky. For a specimen cut from an anisotropic metal sheet, for example, shear deformations are no longer uniform around the circumference (because the shear moduli are different in the longitudinal and transverse directions).

Generally, multiaxial tests on anisotropic materials cannot be interpreted without making reference to a particular modelling scheme. Only the biaxial test along the principal directions of anisotropy is free from this defect.

3.2.2 *Experimental techniques*

Testing machines

The phenomenological method requires the experiments to be made on a volume element of matter. As far as possible the specimens should be subjected to a uniform field of stress, strain and temperature. This is one of the difficulties of mechanical testing for the characterization of materials.

Fig. 3.8. Schematic diagram of a machine for tension–compression tests.

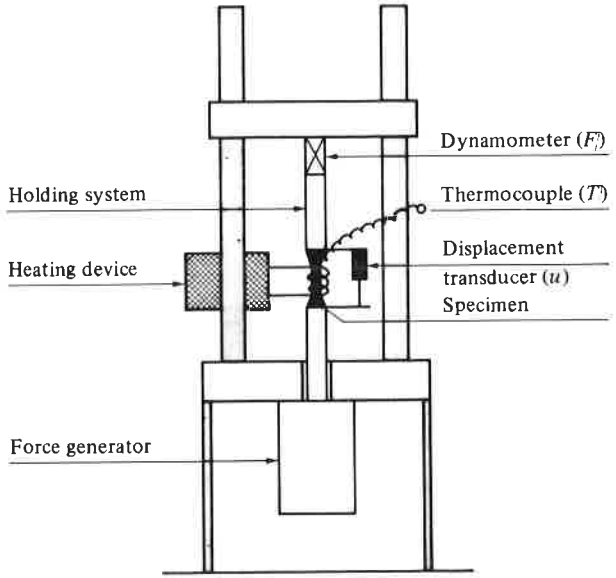

Uniaxial monotonic and cyclic tests

The most common test is the simple tension test in which the useful part of the specimen is subjected to a uniform uniaxial stress field. Fig. 3.8 gives a schematic drawing of a modern set-up, the essential elements of which are as follows:

the system holding the heads of the specimen,
the dynamometer measuring the force applied to the specimen,
the transducer measuring the variation of length of the specimen,
the frame of the machine, which should be as stiff as possible,
the heating device,
the device for applying the forces.

Depending on the type of loading required, the stresses are applied differently: a system of weights for creep testing machines, a continuous screw-nut system driven by an electric motor, a servo-controlled hydraulic system for more sophisticated set-ups. The specimen itself includes a useful part consisting of a cylindrical shaft (Fig. 3.9), end grips, and between the two, shoulders designed to minimize the stress concentration.

For tension tests, the useful part can be very long but is limited by the restriction due to machining and heating devices. In contrast, compression tests require much more compact specimens in order to avoid buckling problems. Actual examples are given later.

For tests at high temperatures either resistance furnaces are used, or the Joule effect (due to the electrical resistance of the sample) or high frequency induction are used to heat the specimen; the latter method is a better one for tests of short or medium duration. The choice of the technique depends on the type of test (monotonic or cyclic) and on the temperatures to be reached (uniform, constant or variable temperature).

Multiaxial tests

In this case tests are conducted to obtain complex stress states in a volume element which could be considered as isostatic. It should be possible to

Fig. 3.9. Specimen for a tension test.

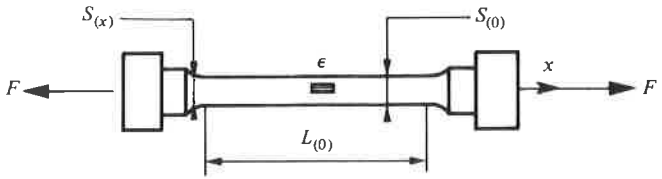

determine the stress state solely by the global equilibrium equations, independent of the material behaviour. Different techniques are used.

Test on cylindrical tubular specimens in tension–compression and internal or external pressure

This is an interesting technique as it does not require special machines. The hydraulic pressurization device (at room temperature) or the gas device (at high temperature) can be adapted to most tension–compression machines. If the wall-thickness e of the specimen is small enough with respect to the radius R, ordinary biaxial states are obtained. Even a pure shear can be simulated ($\sigma_2 = -\sigma_1$) but the principal directions of stress remain fixed (Fig. 3.10). In soil and rock mechanics, this type of test is done with solid (not hollow) samples and with external pressure produced by a pressure cell.

Tension–compression–torsion tests on hollow cylindrical specimens

The possible states of stress are more limited here, but it is possible to study the behaviour for a load path in which the principal directions of

Fig. 3.10. Case of tension–compression – internal pressure and the domain of possible stress states.

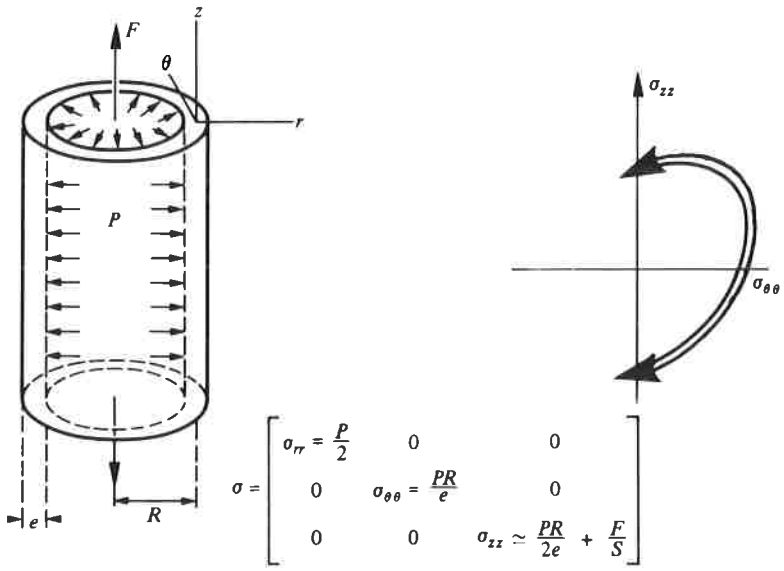

stress are changing (Fig. 3.11). The machine consists of a linear jack and a screw jack with a decoupling device. Modern servo-controlled hydraulic machines are computer driven.

Biaxial tests on cruciform specimens

For this test the machine requires two or four linear jacks placed 90° apart. The transverse bending stiffness of the arms of the cross should be

Fig. 3.11. Case of tension–compression–torsion and the domain of possible stress (C is the twisting couple, J is the torsional moment of inertia of the specimen).

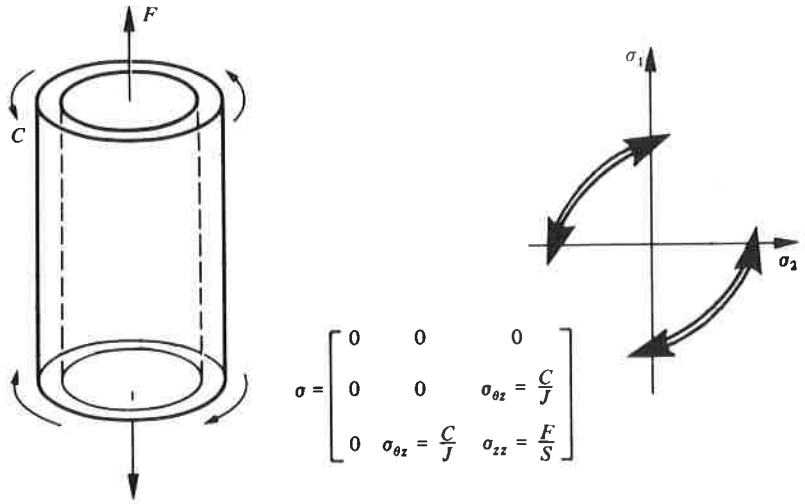

Fig. 3.12. Case of biaxial tension and the domain of possible stress states.

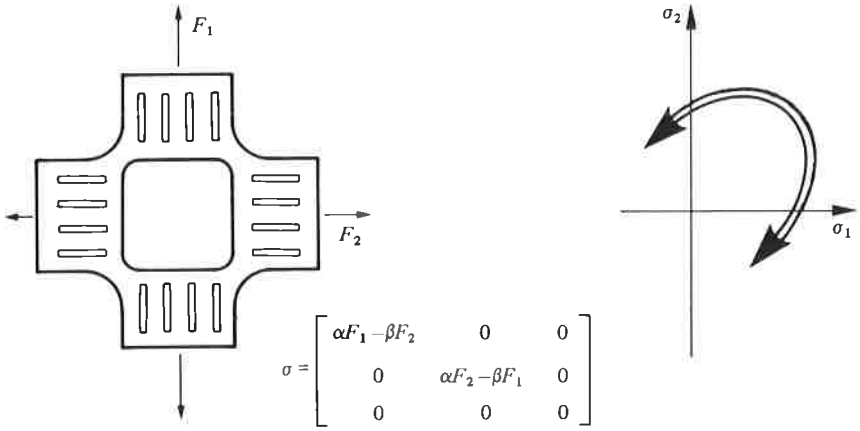

low enough to obtain uniform stress fields. One can, for example, use hollow specimens (Fig. 3.12). The possible loads are such that the principal stresses are positive and their directions remain constant. We may carry out biaxial tension tests on specimens made from plane metal sheets or on specimens in the shape of spherical caps loaded by internal pressure, but then only proportional loading paths can be obtained.

Tests in triaxial compression

This type of test is mostly used in soil and rock mechanics. It requires machines which are delicate to set up.

Techniques of measuring characteristic variables

Forces and stresses

Stresses can be deduced from forces by static equations for isostatic cases. Three examples are given in Figs. 3.10–3.12.

The forces (or couples) applied to the specimens are measured by dynamometers mounted in series with the specimens. The dynamometers, equipped with strain gauges, have a relative precision of 10^{-3} which is generally sufficient for the characterization of materials.

Displacements and strains

The measurement of relative displacement between two points on a specimen is a much more delicate operation than the measurement of the loading force. To measure relative displacement it is necessary to connect a strain gauge in 'parallel' with the sample and not in series. Essentially two techniques are used: local measurements by electrical resistance strain gauges, and global displacement measurements.

Wire strain gauges

A resistance wire, well glued to the specimen, experiences the same strain as the specimen. It therefore follows that the variation in electrical resistance will be proportional to the strain ε. A precise measurement of this variation in resistance is obtained by employing a Wheatstone bridge; this can detect strains of the order of $\varepsilon = 10^{-7}$. However, the qualification 'well glued' mentioned above limits the applicability of this particularly useful technique. Adhesives do not withstand high temperatures, and hence, these strain gauges are only used at, or below, room temperature, or at slightly higher temperatures (not more than 200–400 °C).

Displacement transducers

The strain can also be deduced from the equations of continuum mechanics and knowledge of the displacement between two material points of the specimen. The axial displacement can be measured by an extensometer attached either to the cylindrical part of the specimen through knife edges, or to the gripping heads of the specimen. The variation in the diameter of the specimen can also be measured but without using the knife edges which very often initiate a fracture. The evaluation, however, must take into account the variation of Poisson's coefficient in the presence of plastic strains (see Section 3.2.1). With inductive extensometers or with strain gauges, an absolute precision of 1 μm can be attained. With optical extensometers this precision can be improved to 0.2 μm, but these are expensive and delicate instruments.

Plastic deformation. Useful lengths of specimens

The useful length of a sample is the length L_0 which becomes L under the load, and which can be used to calculate the longitudinal strain by the simple relation:

$$\varepsilon = (L - L_0)/L_0.$$

The plastic strain can be obtained by subtracting the elastic strain from the total strain ε (measured, for example, by an electric resistance strain gauge). In tension (compression) we then have:

$$\varepsilon_p = \varepsilon - \varepsilon_e = \varepsilon - \sigma/E = \varepsilon - F/ES$$

where S is the current cross-sectional area of the specimen.

The modulus of elasticity is obtained from data at the beginning of the test when the force is sufficiently low for the specimen to remain elastic. We then obtain:

$$E = F/S\varepsilon_e.$$

When the extensometer cannot be connected directly onto the cylindrical part of the specimen, we take an equivalent useful length L_p corrected to take into account the plastic deformations in the connection areas. Employing the notation of Fig. 3.9, this is defined by:

$$L_p = \frac{u_p}{\varepsilon_{p(0)}} = 2\int_0^{L/2} \frac{\varepsilon_{p(x)}}{\varepsilon_{p(0)}}\,dx.$$

It will be seen in Chapter 5 that the plastic strain can be expressed as a power function of the stress $\varepsilon_p = (\sigma/K)^{1/M}$. By a method of slicing, and

neglecting the triaxiality effect in the connection zones, we can easily show that:

$$L_p = 2\int_0^{L/2} \left(\frac{S_{(0)}}{S_{(x)}}\right)^M dx.$$

The useful plastic length is thus defined from the geometry of the specimen (law of variation of section $S_{(x)}$) and the hardening exponent. The procedure used to measure the plastic strain is therefore the following:

determine the force–displacement relation by direct readings in a tension test (for example),
subtract the initial displacement u_j and the elastic displacement to obtain the plastic displacement. The stiffness R of the specimen and the grips at the level of the extensometer is obtained from the initial readings in the elastic domain (Fig. 3.13). Then:

$$u_p = u - u_j - F/R.$$

The relation $F(u_p)$ furnishes an approximation to the hardening

Fig. 3.13. Direct recording of a hardening test.

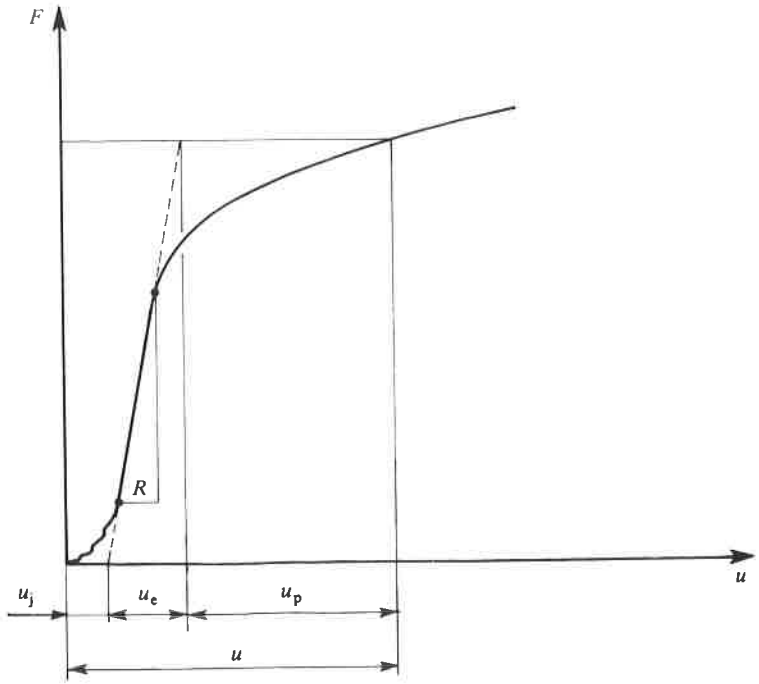

exponent M. In fact, an identity exists between the exponents of the power laws:

$$\sigma = K\varepsilon_p^M \quad \text{and} \quad F = K'u_p^M$$

since

$$\sigma = F/S \quad \text{and} \quad \varepsilon_p = u_p/L_p.$$

The equivalent useful length L_p can be derived from these equations, and hence,

$$\varepsilon_p = u_p/L_p.$$

It should be noted that this useful length can be defined by a preliminary test for a given specimen, material, and temperature. Even if the hypotheses used to establish it are not completely rigorous, they are sufficient since the correction is, in fact, small with respect to the length of the cylindrical zone.

Temperature

The most commonly used technique for measuring temperature involves the use of thermocouples: these measure the electromotive force which arises due to the Pelletier effect between a 'hot' soldering of two wires, such as chromium and aluminium ones for example, with both ends at the same reference temperature.

When equipment sensitive to measurements in microvolts is available, the theoretical precision of a chromium–aluminium thermocouple is 2.5×10^{-2} °C. This precision is quite adequate for characterization tests of materials for which an absolute precision of the order of ± 0.1–0.5 °C can be satisfactory. The most critical condition occurs for viscoplastic behaviour. A calculation based on the Dorn relation presented in Chapter 6 expresses the rate of the plastic strain as a function of temperature:

$$\dot{\varepsilon}_p = f(\sigma, \ldots)\exp(-\Delta H/kT).$$

This relation can be used to show that the desired relative precision of temperature measurements must be of the order of 15–70 times more than that for the measurement of strains:

$$\delta\varepsilon_p/\varepsilon_p \approx 15 \text{ to } 70(\delta T/T).$$

A strain measurement with a level of precision of 2% at 500 °C requires a uniform temperature throughout the specimen within a tolerance of approximately 0.5 °C.

The thermocouples must be welded onto the specimen but this weld constitutes a site for fracture initiation. Consequently, thermocouples can be used only for tests designed for the study of deformation behaviour. In the case of static fracture tests or fatigue fracture tests, we may employ optical transducers which measure infrared emission from the sample. This, however, has a drawback in that the emission power of the specimen varies with its state of damage.

Damage

It will be seen in Chapter 7 that global measures of damage involve only the evaluation of stresses and strains as functions of time or the number of cycles.

Crack length or crack surface

The measurement of crack length or of crack surface is often a delicate task as the crack-tip or the crack-front is not always well defined physically, and corresponds to highly damaged zones full of microcracks.

Optical measurement

This measurement is performed by direct visual means – more precisely, by a photographic process: a camera with an automatic tripping mechanism sends an image at regular intervals. After processing and enlarging the images (reference marks are needed in the working zone to provide a scale) the crack length is obtained by direct measurement. The precision of the result depends on the illumination, enlargement, quality of the reference marks and good definition of the crack-tip. The precision varies between 0.05 and 0.01 mm.

Gauges with cut wires

These consist of wires glued on a support at a spacing of 0.5–1 mm. The support itself is then glued in front of the tip of the crack whose length is to be measured. As the crack grows, it cuts the wires one after the other. This results in a variation of the resistance of the gauge or in an incremental signal that activates a recording device. The precision of this system without interpolation is of the order of the spacing between the wires.

Method of potential drop

The specimen or cracked element, which should be conducting but insulated, is powered continuously, at a point far from the crack, by an electric current of high intensity (≈ 20 A), preferably a direct current. A

potential plug with its two points on either side of, and close to the crack, measures a potential difference V which is a function of the dimensions of the specimen, of the location of the current supply, of the potential plug, and of the crack length a. A measurement of V therefore permits the determination of a, if the function $a(V)$ is known either through a preliminary calibration done with another means of measurement, or by calculation. A diagram of this measurement technique is given in Fig 3.14. Even though the potential difference to be measured is very low, of the order of tenths of a microvolt, the precision of the measurement can reach a few hundredths of a millimetre for crack lengths measured in thin metal plates, provided that the measurement is synchronized with the maximum opening of the crack.

This method can also be applied to measure the depths of noncrossing crack-fronts in massive parts. The calibration, although more complex, can be done using a rheo-electrical analogy tank; in this case, the precision is of the order of tenths of a millimetre in measuring the coordinates of each point of the crack-tip.

Specimens

The preparation of the specimens is always a long and delicate task as, unless care is taken, fracture can occur prematurely and not precisely where it is expected! It always involves a compromise between the implications of the machine characteristics (loading type, maximum force, stiffness, heating

Fig. 3.14. Diagram showing fatigue crack length measurement by the potential drop technique (after Baudin and Policella).

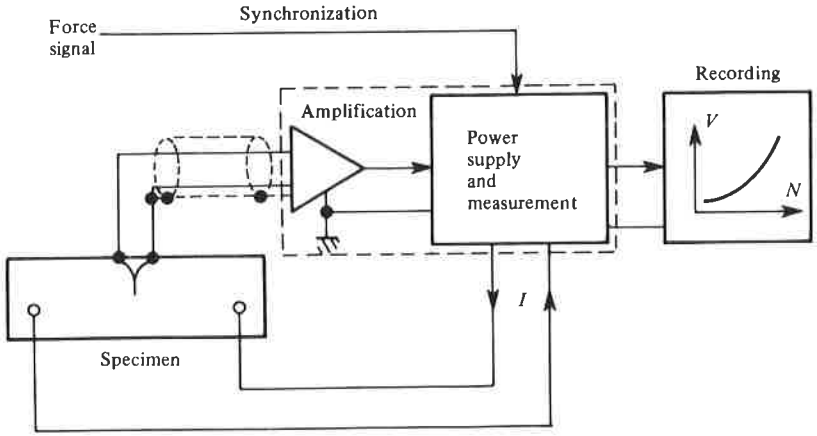

system) and the implications of the measurements to be carried out (sensitivity of the dynamometers, elongation measurements by extensometers placed locally on the useful part of the specimen or externally on the gripping heads). A few examples of dimensioned drawings which have

Fig. 3.15. Specimens for tension tests ((*a*) with a circular cross-section, (*b*) flat) and tension–compression tests ((*c*) for an external extensometer or strain gauge, (*d*) for a local or optical extensometer).

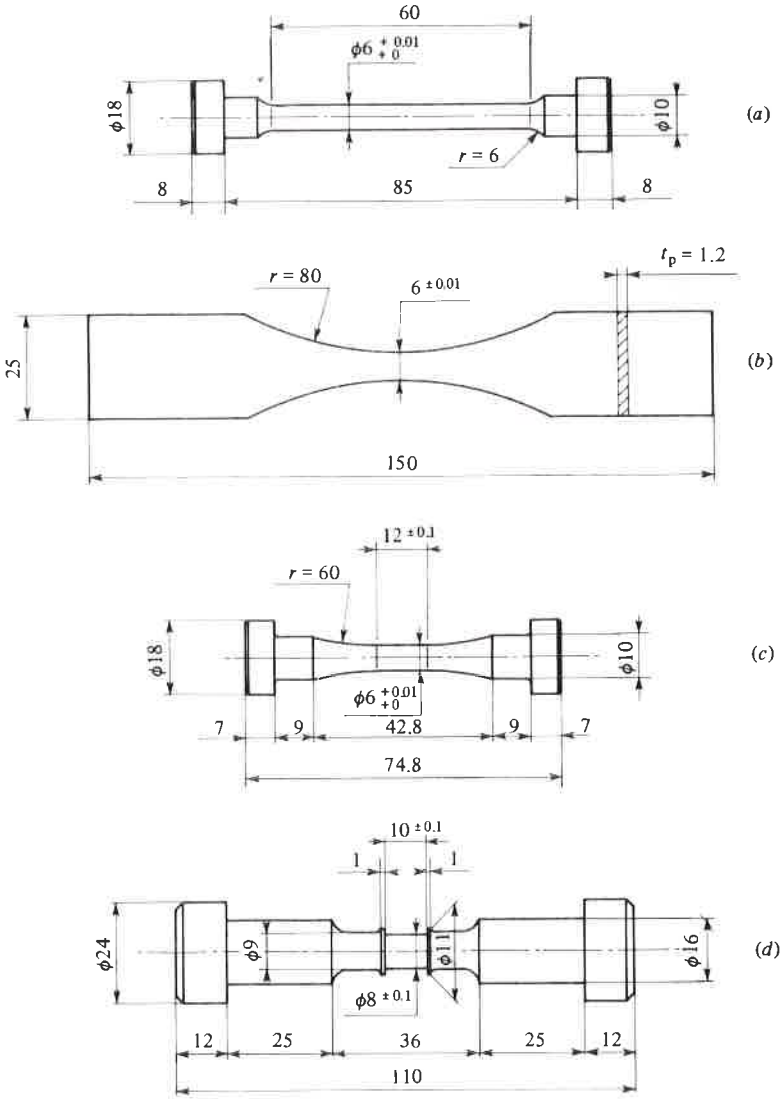

proved to be reliable are given in Figs. 3.15–3.19 (after Dauzou, LMT Cachan).

3.2.3 *Identification methods*

Thermodynamics gives the general formulation of models without specifying their analytical form (except, however, for linear behaviour) or numerical values. On the other hand, experiments provide, for each material, the quantitative relations to be verified by the models constructed to represent the phenomena under study. Identification can be defined as all the work which consists in specifying the functions which appear in the model and in finding the numerical values of the coefficients which define the functions for each material.

Fig. 3.16. (*a*) Specimen for tension. (*b*) Specimen for pure shear in compression.

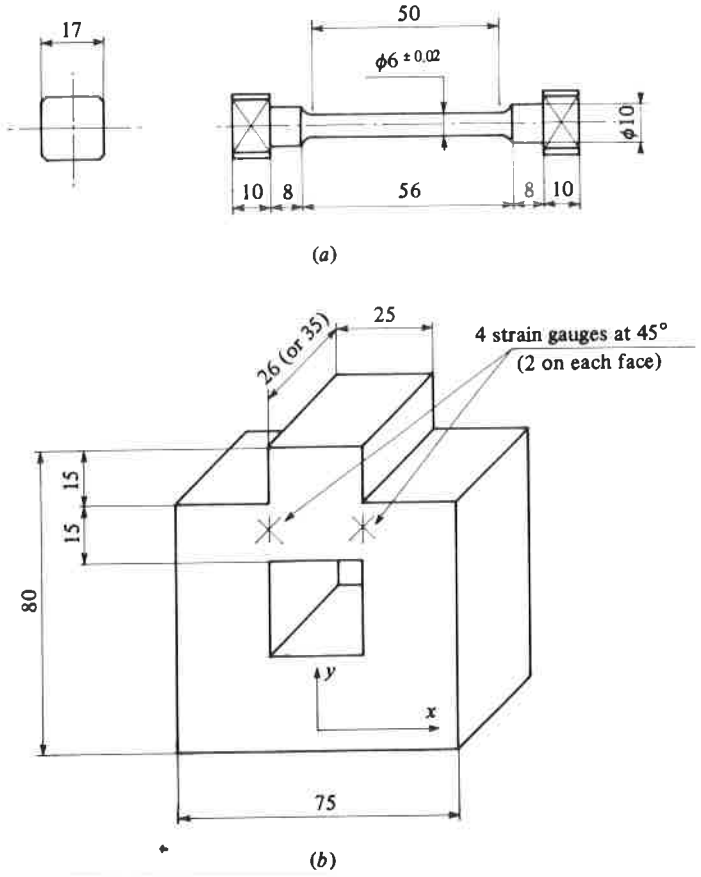

This represents a difficult task which does not follow any rigorous rules and in which experience and 'art of model construction' play a major role in steering between theory and experiment.

Analytical formulation of models

The ratio of quality versus price

Given a set of experimental results, it is always possible to find a function which represents it with an error not greater than the margin of uncertainty in measurements. This is called fitting. Since the number of experimental

Fig. 3.17. Specimen for tension–torsion. (*a*) Fixation by pins. (*b*) Fixation by clamping.

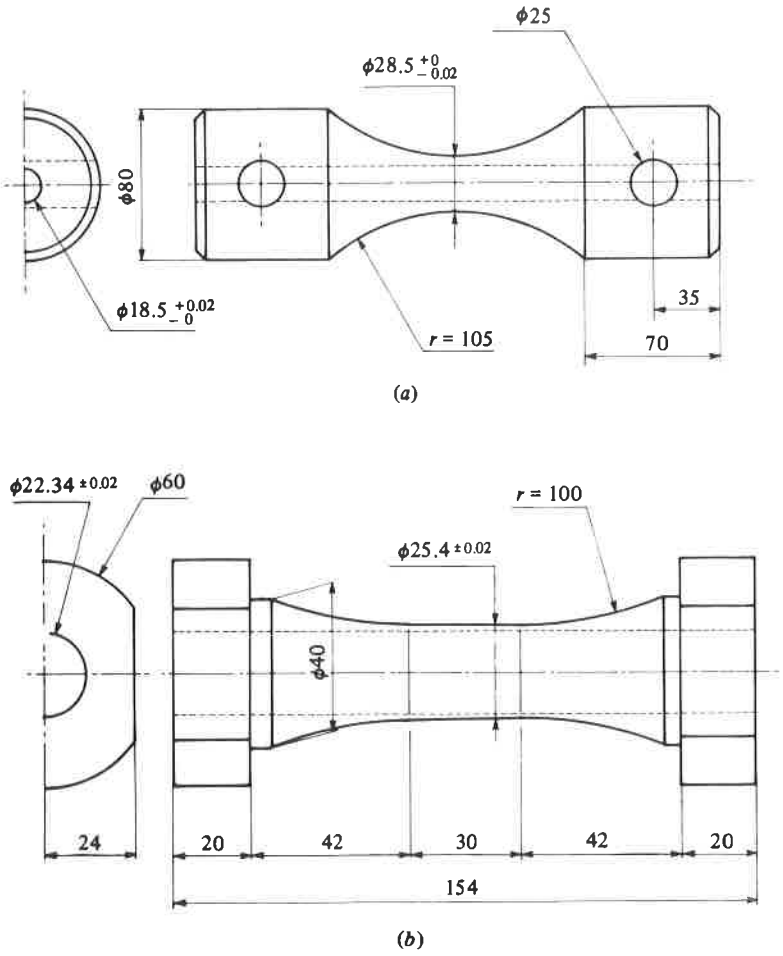

points can be large, the fitting may require functions with a large number of representative coefficients.

On the other hand, a model which has the ambition of becoming a law, must possess a general character, so that while identified only by a restricted number of experiments, it is representative of other types of experiments with a predictive capability. The totality of the situations verified by a model is its field of validity. This characterizes the goodness of the model and is expressed qualitatively by the set of all possible variation histories of the variables and quantitatively by the range of the variations within which the model agrees with the physics. For example, the Hencky–Mises plasticity law (Chapter 5) is valid for an isotropic material under radial loading up to strains lower than the damage threshold (Chapter 6).

The number of coefficients represents the price to pay since the difficulties of identification essentially lie in this number. It may be easy to identify say two coefficients by a 'hand procedure', but the identification of say five coefficients in a model will involve considerable numerical work; and the identification of say ten of them really belongs to 'computer-aided art'.

Fig. 3.18. (*a*) Specimen for ductile damage test. (*b*) Specimen for fatigue test.

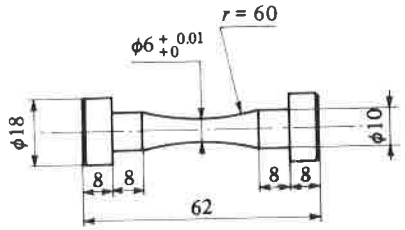

(*a*)

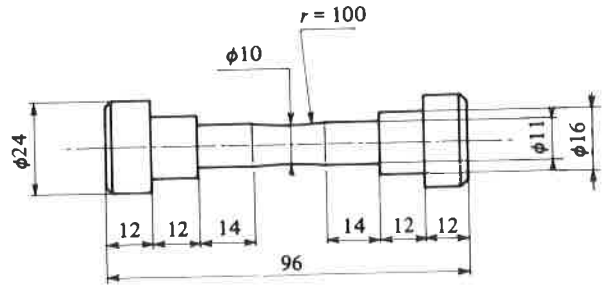

(*b*)

Therefore, to evaluate a model it is necessary to examine this relation of quality/price = domain of validity/number of coefficients clearly.

Modelling of nonlinearities

Most of the phenomena studied in this book (plasticity, viscoplasticity, damage, cracking) are 'very strongly' nonlinear, in the sense that a linearization limited to the first order Taylor expansion represents the phenomenon only for a very small change in the variables.

Among all the analytical possibilities for representing nonlinearities, the following will be considered:

the exponential: $\exp(aX)$, or the logarithm $\ln(aX)$,
the power function aX^N where N is a coefficient which may take the

Fig. 3.19. Crack specimens. (*a*) ASTM CT specimens. (*b*) Irwin specimen.

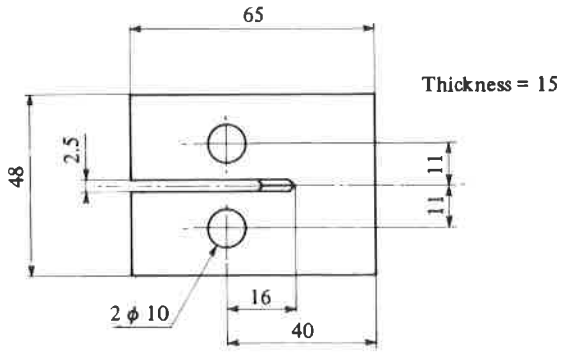

(*a*)

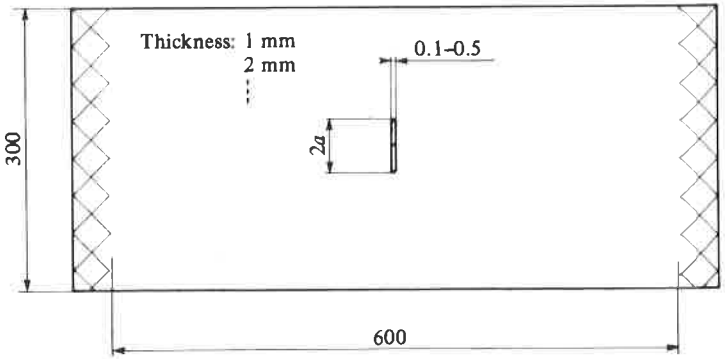

(*b*)

values, 2, 5, 10, 20 or even 100. In some cases it is necessary to use the function $aX^{N(X)}$ in which N itself is a function of X.

The reasons for this are essentially twofold:

the easy identification by logarithmic transformation which yields linear relations,
the possibility of obtaining analytical solutions of models for studying their properties.

Rule of linear accumulation

An important property, whether or not satisfied in a model, is the rule of linear accumulation (for example, the Robinson rule for creep and the Palmgreen–Miner rule for fatigue) which, in fact, is a property common to any differential equation, linear or nonlinear, which admits separation of variables.

Models resulting from dissipation potentials (see Chapter 2) always have the general form:

$$\dot{X} = f(X, V(t))$$

where X is the evolution variable of the phenomenon and is a function of the causal variables V (taken here to be just one variable for simplicity).

Let us show that if this differential equation admits separation of variables:

$$\dot{X} = g(X)h(V)$$

(where g and h may be nonlinear functions), then it implies the rule of linear accumulation. For the initial condition $X = 0$ at $t = 0$, the solution of this equation can be expressed as:

$$[g(X)]^{-1}\,\mathrm{d}X = h(V)\,\mathrm{d}t$$

or

$$\int_0^X [g(x)]^{-1}\,\mathrm{d}x = \int_0^t h(V)\,\mathrm{d}t.$$

Consider first the case where V is constant equal to V_0. The corresponding solution $t(X, V_0)$ is:

$$t(X, V_0) = [h(V_0)]^{-1} \int_0^X [g(x)]^{-1}\,\mathrm{d}x.$$

Consider now the case where V varies with time and let:

$$\tau(X, V) = [h(V)]^{-1} \int_0^X [g(x)]^{-1}\,\mathrm{d}x$$

be a function of X and the time derived from $t(X, V_0)$ by replacing V_0 with $V(t)$. Since $\mathrm{d}t = [h(V)]^{-1}[g(X)]^{-1}\,\mathrm{d}X$, let us calculate:

$$\int_0^{t^*} \frac{\mathrm{d}t}{\tau(X^*, V(t))}$$

where t^* is the time which corresponds to X^*, i.e., $X^* = X(t^*)$. We have:

$$\int_0^{t^*} \frac{\mathrm{d}t}{\tau(X^*, V(t))} = \int_0^{t^*} \frac{[h(V)]^{-1}[g(x)]^{-1}\,\mathrm{d}x}{[h(V)]^{-1} \int_0^{X^*} [g(x)]^{-1}\,\mathrm{d}x}$$

$$= \int_0^{X^*} \frac{[g(x)]^{-1}\,\mathrm{d}x}{\int_0^{X^*} [g(x)]^{-1}\,\mathrm{d}x} = 1.$$

Hence,

$$\int_0^{t^*} \frac{\mathrm{d}t}{\tau(X^*, V(t))} = 1.$$

This relation expresses the fact that the accumulation of the time ratio $\mathrm{d}t/\tau$ is equal to 1. Here τ is the solution obtained by considering a constant process instead of the variable process signified by $V(t)$.

This is the linear accumulation rule which applies to all separable differential equations. For example, in fatigue, Miner's rule for a variable loading amplitude of stress $\Delta\sigma(N)$ is:

$$\int_0^{N_R} \frac{\mathrm{d}N}{N_F(\Delta\sigma(N))} = 1$$

where N_R is the number of cycles to fracture for the type of loading considered and N_F is the reference number of cycles to fracture for a periodic loading of range $\Delta\sigma$.

Scatter and randomness in coefficients

Another important aspect is the scattering of the experimental results. This can be due to:

the nature of the phenomenon, inhomogeneities, random growth processes, load uncertainty,

the inherent scattering in each sample arising from the production or casting process and also from the heat treatment, and so on....

Usually, scattering is of the order of 1–5% for elastic strains, 10–50% for plastic or viscoplastic strains, 50–100% (factor of 2) of the number of cycles for low cycle fatigue crack initiation or growth, and 1000% (factor of 10) for fatigue failure in the high cycle regime.

These orders of magnitude of scattering indicate at once the pronounced influence of nonlinearities of the phenomena. The simplest and most efficient way of including this scattering in a model consists in giving a statistical definition to the multiplying coefficients present in the model, for example the coefficient A in:

$$\dot{X} = AX^m V^n.$$

With sufficient experimental results, it is possible to define A by its probability density, or by the probability distribution curve, or often just by its mean value and standard deviation.

Fig. 3.20 shows the viscoplastic behaviour of the alloy INCO 718 at 550 °C, observed through the viscosity and hardening functions (see Chapter 6). The scattering from one sample has an effect on the ordinates, i.e. on the stress, but not on the nonlinearity of the two functions.

Using $M = 13$ and $N = 140$ for a larger number of tests, it has been possible to derive the statistical distribution of the strength coefficient K of the viscoplastic law:

$$\sigma = K\varepsilon_p^{1/M}\dot{\varepsilon}_p^{1/N}.$$

Fig. 3.20. Identification of the coefficients of the viscous-hardening law for INCO 718 alloy at 550 °C.

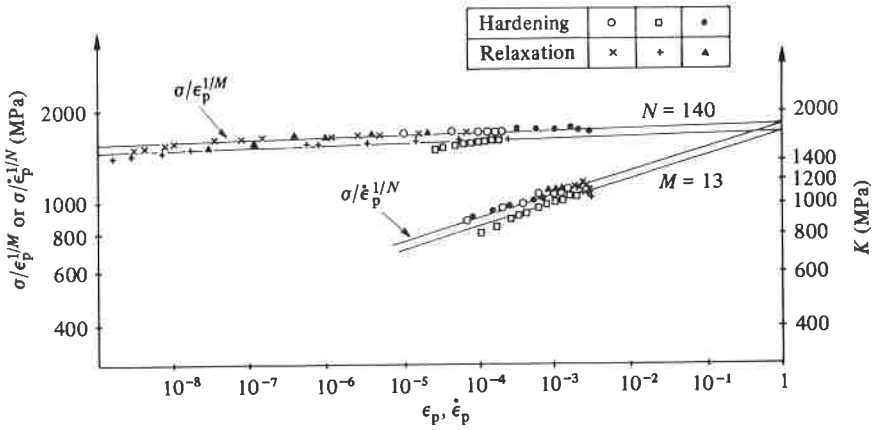

Fig. 3.21 shows that this distribution is very close to the distribution observed for the conventional yield stress (at 0.2% permanent strain).

Numerical methods of identification

Knowing a mathematical model by its analytical expression, and obtaining a set of experimental results in which all the variables of the model have been activated, we are in a position to calculate the unknown coefficients which give the best representation of the experimental results.

Generalities

Let us mention at once that problems arise differently depending on the test data available and the model under study. Two cases have to be distinguished.

The constitutive law is directly identified, i.e., we seek the entity (or the transfer function) representative of the material. One example of this is a law in which a variable X and its derivative $\dot{X}$ are present:

$$H(X, \dot{X}, Y) = 0$$

Fig. 3.21. Probability densities for the $\sigma_{0.2}$ yield stress and for the strength coefficient K of INCO 718 alloy at 550°C.

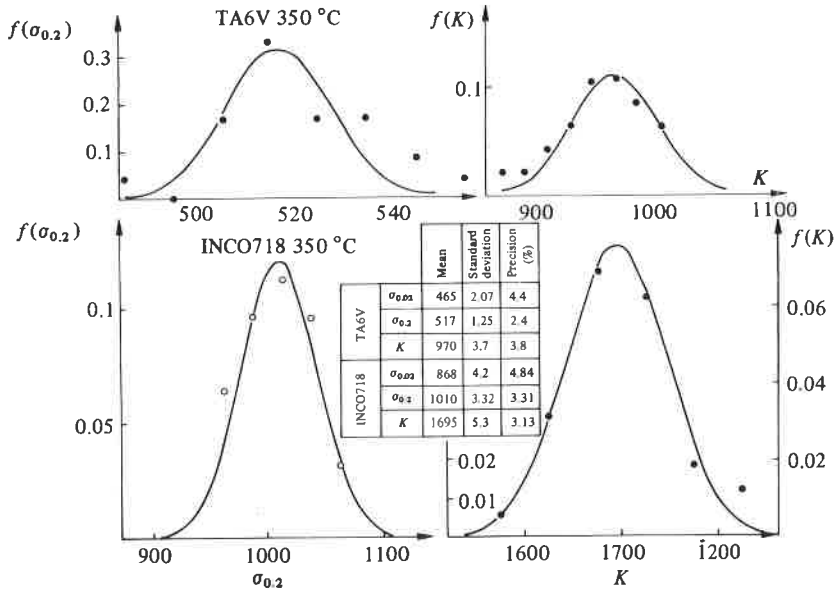

Once a series of triplets of values $(X, \dot{X}, Y)$ have been measured (at the same instant), the coefficients which define the above function H can be obtained by direct fitting of the experimental points. Depending upon the particular case, we may use a linear or nonlinear least-squares method to obtain these coefficients (see below).

The response is identified, i.e., the coefficients of the function H are determined by adjusting, in the best possible way, the response values obtained from the assumed constitutive equation for a given load (input) against values obtained experimentally under the same load. In this case we use a nonlinear least-squares method, since the response cannot usually be stated explicitly in a simple analytic way.

Remarks

A given model cannot be identified correctly unless a sufficient number of test results are available which embrace a significant range of variation of each of the parameters (for example, the parameters X, $\dot{X}$ and Y in the above function H). Otherwise, we run the risk of not determining one or more coefficients well enough.

For an identical material and model, it may be necessary to define several sets of coefficients, each better suited to a domain of variation or to a load type, for example, rapid transient loads, short-term loads, long-term loads and stationary loads.

Linear least-squares method

Our objective is to minimize the discrepancy between the experimental data and the theoretically calculated values from a model. Different norms may be used, and generally speaking, we have the problem of minimizing an error function:

$$h(a)$$

which depends on the unknown coefficients a_i $(i = 1, 2, \ldots, n)$. Different methods of minimization can be used. They have different efficiencies; however, in general, convergence may be difficult to achieve, due to large nonlinearities of the phenomena generally studied. We limit ourselves here to presenting the linear least-squares and Gauss–Newton methods when the error function is chosen as the sum of the squares of the discrepancies:

$$h(a) = \tfrac{1}{2} \sum_{j=1}^{m} E_j^2 = \tfrac{1}{2} \sum_{j=1}^{m} [y_j^{\mathrm{C}}(a, x_j) - y_j^{\mathrm{E}}(x_j)]^2.$$

y_j^{E} and y_j^{C} represent respectively the experimental and the calculated values of one of the parameters as a function of the others denoted by x_j (jth experimental point). Fig. 3.22 illustrates in a schematic way how this function is defined.

The linear least-squares method is used when the expression for y^{C} is a linear function of the coefficients a_i:

$$y_j^{\mathrm{C}} = A_0(x_j) + A_1(x_j)a_1 + \cdots + A_n(x_j)a_n.$$

To minimize h it is sufficient to require that:

$$\partial h / \partial a_k = 0 \quad \forall k = 1, 2, \ldots, n$$

Then, since h is quadratic we immediately find, with $A_{ij} = A_i(x_j)$:

$$\sum_i \left(\sum_j A_{jk} A_{ji} \right) a_i = \sum_j A_{jk}(y_j^{\mathrm{E}} - A_0).$$

The solution of this system of linear equations, whose matrix is symmetric, easily furnishes the unknown a_is.

Gauss–Newton method

This is a generalization of the preceding method. For a nonlinear expression of a function, y^{C}, we introduce the linearization:

$$y_j^{\mathrm{C}}(a) = y_j^{\mathrm{C}}(a^0) + \sum_{i=1}^{n} \frac{\partial y_j^{\mathrm{C}}}{\partial a_i}(a^0) \Delta a_i$$

Fig. 3.22. Identification graph.

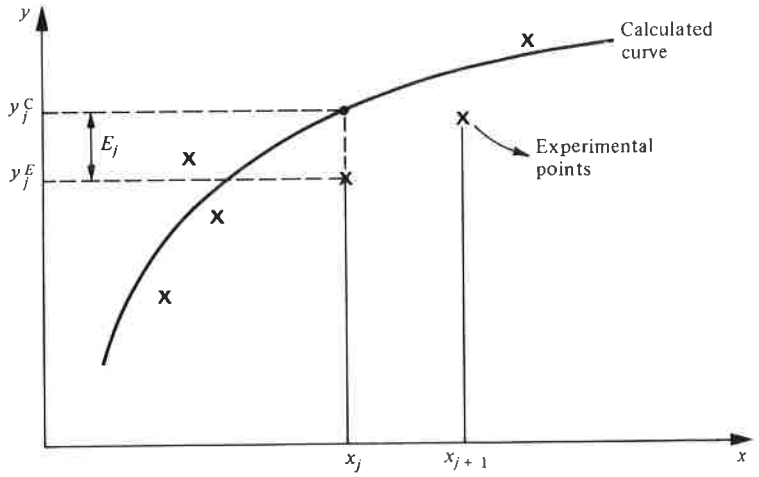

For a given set of coefficients a^0, the error function at each point y_j^C and its derivative with respect to each of the coefficients is calculated (these gradients can rarely be determined explicitly and it is generally necessary to proceed with small finite increments of each coefficient). This expression is formally identical to the expression in the previous section. To obtain a set of values Δa_i, that generally leads to an acceptable solution, it is sufficient to replace a^1 by:

$$a_i^1 = a_i^0 + \Delta a_i.$$

From this new solution, we again proceed in the same way. Note that, the convergence of this iterative method is not always certain. However, when it does converge, it does so rapidly. This means that the method is easy to use and relatively inexpensive if the number of coefficients remains small.

Fig. 3.23 shows the example of identification of the plasticity law for 316 L steel by a tension test conducted at 20 °C. The chosen equation contains three coefficients:

$$\sigma = \sigma_Y + K_Y \varepsilon_p^{1/M_Y}$$

Fig. 3.23. Identification of a three coefficient plasticity equation for 316 L steel.

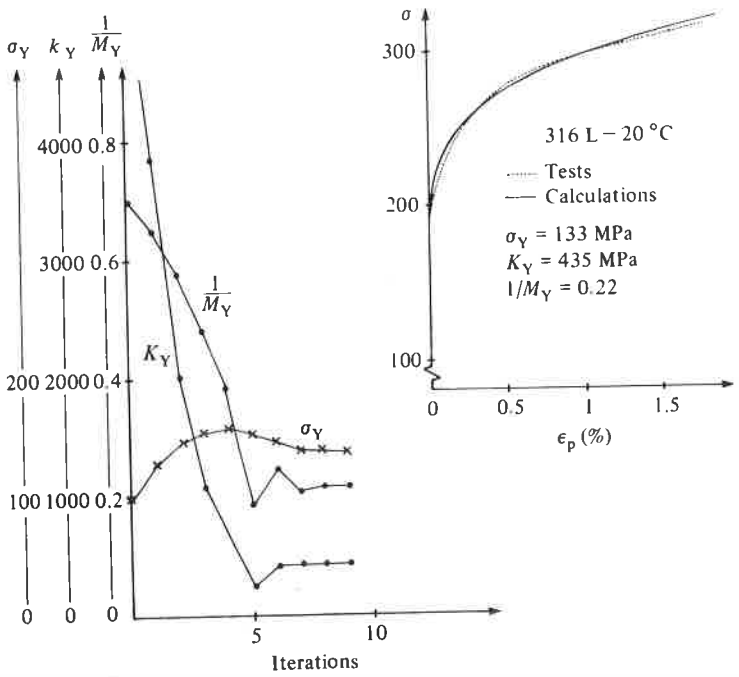

and we find that for different starting solutions, the convergence is sufficiently fast and accurate.

Variation of characteristic parameters as a function of temperature

Notwithstanding the exceptions, the characteristic parameters of a material that define each constitutive model depend on the temperature. A general method which allows us to introduce this dependency consists in writing these coefficients in the form of a parabolic function which is defined piecewise. For example, for the parameter α, let:

$$\alpha(T) = a_i(T - T_i)^2 + b_i(T - T_i) + c_i \quad \text{for} \quad T_i < T < T_{i+1}.$$

The coefficients a_i, b_i, c_i are chosen in such a way as to ensure the continuity of α and $d\alpha/dT$:

$$c_{i+1} = a_i(T_{i+1} - T_i)^2 + b_i(T_{i+1} - T_i) + c_i$$
$$b_{i+1} = 2a_i(T_{i+1} - T_i) + b_i.$$

They are determined step by step, by the measured values of the parameter α, and by eventually introducing intermediate values to ensure a good fit.

3.3 Schematic representation of real behaviour

The qualitative aspect of the response of materials to characteristic tests allows us to classify them by the following adjectives: rigid, elastic, viscous, plastic and perfectly plastic. To each particular type there corresponds a mathematical theory developed in Chapters 4–8.

3.3.1 *Analogical models*

Analogical models are assemblies of mechanical elements with responses similar to those expected in the real material. They are used, very often for didactive purposes, to provide a concrete illustration of the constitutive equations. The analogy stops there and never concerns itself with the physical mechanisms themselves.

The most commonly used elements are the following:

the spring to represent linear elasticity

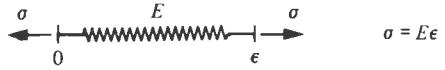

the damper to represent linear or nonlinear viscosity

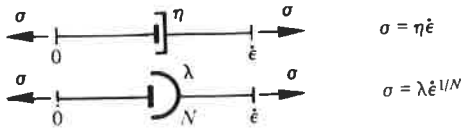

the skidding block to represent a stress threshold

the stopping block to represent a strain threshold

These different elements (index i) may be assembled:

either in series:

$$\varepsilon = \sum_i \varepsilon_i \qquad \sigma = \sigma_i$$

or in parallel:

$$\sigma = \sum_i \sigma_i \qquad \varepsilon = \varepsilon_i$$

or in mixed groupings.

Using electro-mechanical analogies these models can also be realized as electrical networks but numerical calculations have replaced these analog devices.

3.3.2 *Rigid solid and perfect fluid*

These are only mentioned as a matter of interest as they do not belong to the mechanics of deformable solids. In practice, the distinction between solids and fluids is a subjective one, and it can only be linked to the choice of a time scale:

a solid admits a state of equilibrium under load;
a fluid undergoes a flow for any load even for a very small one.

It is not easy to differentiate between an infinitely slow flow and an equilibrium reached in an infinite time! The ambiguity can be resolved by using a time scale linked to the phenomenon under consideration. But then,

the notions of fluid and solid lose their objective meaning: it is possible to consider a given polymer as a solid for shock problems and as a fluid for problems of long-term stability.

3.3.3 *Viscous fluid*

A body is called a 'viscous fluid' if its response to characteristic tests is of the type shown in Fig. 3.24. Sometimes such a body is also called a viscoplastic solid (see Chapter 6).

There is flow for any value of stress $\dot{\varepsilon} = f(\sigma)$.

A simple analogical model is the Maxwell model which consists of a linear spring and a damper in series. Its constitutive equation is:

Its response to a relaxation test $\varepsilon = \varepsilon_0 H(t)$ where $H(t)$ is the Heaviside step function, $H = 0$ if $t < 0$ and $H = 1$ if $t \geqslant 0$, is:

$$\sigma = E\varepsilon_0 \exp\left(-\frac{E}{\eta}t\right).$$

Application to 'soft' solids: thermoplastic polymers in the vicinity of their melting temperature, fresh concrete (neglecting its ageing), numerous metals at a temperature close to their melting point.

3.3.4 *Elastic solids*

The deformation of elastic solids is essentially reversible. A detailed study of these solids is presented in Chapter 4.

Fig. 3.24. Viscous fluids.

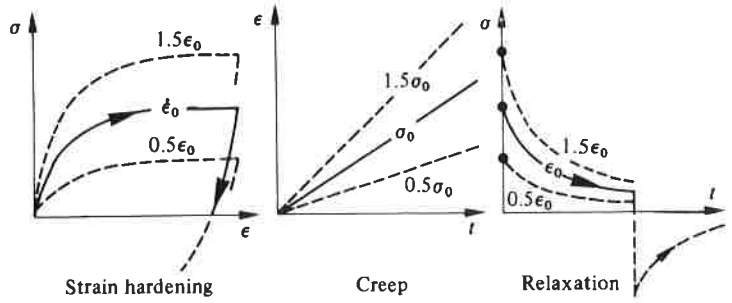

Perfectly elastic solid

The qualitative responses of a perfectly elastic solid to three characteristic tests are as shown in Fig. 3.25.

The reversibility is instantaneous. The stress–strain relation is:

$$\sigma = f(\varepsilon).$$

The analogical model of the linear elasticity is the spring:

$$\sigma = E\varepsilon.$$

Applications: metals, concrete, rocks loaded below the elastic limit.

Viscoelastic solid (Fig. 3.26)

The recovery of deformation is 'delayed' and is achieved only after an infinite time:

$$\sigma = f(\varepsilon, \dot{\varepsilon}).$$

Fig. 3.25. Perfectly elastic solid.

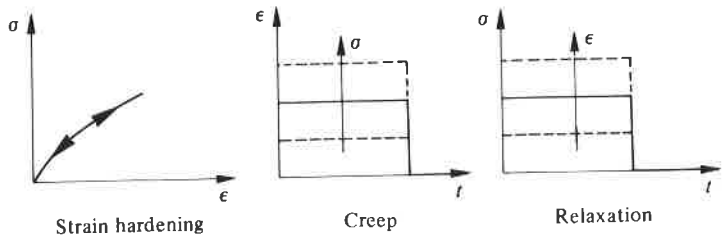

Fig. 3.26. Viscoelastic solids.

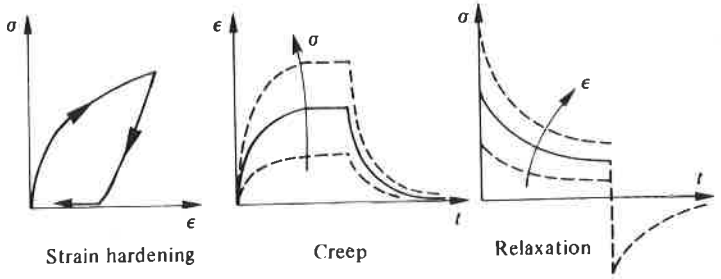

A simple analogical model is the Kelvin–Voigt model which consists of a linear spring and a damper connected in parallel:

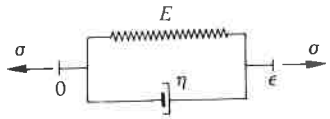

Its response to a creep test $\sigma = \sigma_0 H(t)$ is:

$$\varepsilon = \frac{\sigma_0}{E}\left[1 - \exp\left(-\frac{E}{\eta}t\right)\right].$$

The generalized analogical models of Kelvin–Voigt and Maxwell for solids are described in Chapter 4. Viscoelastic solids often exhibit the phenomenon of ageing; this point is discussed in Section 3.3.8.

Applications: organic polymers, rubber, wood when the load is not too high.

3.3.5 *Plastic solids*

Plastic solids are those which after the application of a load reveal instantaneously stable permanent deformations and which are in equilibrium with the load. Their behaviour is not explicitly related to time.

By definition, the plastic strain ε_p is that which corresponds to the relaxed configuration $\varepsilon_p = \varepsilon(\sigma = 0)$. Chapter 5 is devoted to a detailed study of plastic solids.

Rigid perfectly plastic solid (Fig. 3.27)

The strain is either zero or negligible until a stress threshold σ_s is reached and is arbitrary at this value of stress, independent of the strain rate $\dot{\varepsilon}$ in a

Fig. 3.27. Rigid perfectly plastic solid.

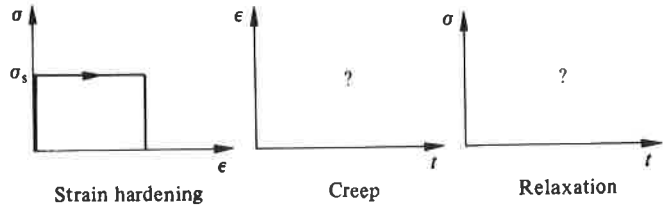

hardening test or time in a creep or a relaxation test:

$$|\sigma| < \sigma_s \rightarrow \varepsilon = 0$$
$$\sigma = \sigma_s \operatorname{Sgn}(\dot{\varepsilon}) \rightarrow \varepsilon = \varepsilon_p \qquad \text{(arbitrary)}$$

The analogical model is a skidding block.

Applications: soil mechanics, analysis of metal forming (cf. Chapter 5).

Elastic perfectly plastic solid (Fig. 3.28)

The strain is linear elastic before the threshold σ_s is reached. Thereafter, the strain is arbitrary and independent of the strain rate for this value of stress:

$$|\sigma| < \sigma_s \rightarrow \varepsilon = \varepsilon_e = \sigma/E$$
$$\sigma = \sigma_s \operatorname{Sgn}(\dot{\varepsilon}) \rightarrow \varepsilon = \varepsilon_p \qquad \text{(arbitrary).}$$

The analogical model for an elastic, perfectly plastic solid is the Saint–Venant model consisting of a linear spring in series with a skidding block:

Applications: steels with a low carbon content (i.e., those exhibiting a plateau) for $\varepsilon < 2 \times 10^{-2}$ and $T < \frac{1}{4} T_M$ (where T_M is the melting temperature in K), limit analysis (cf. Chapter 5).

Elastoplastic hardening solid (Fig. 3.29)

The total strain is the sum of a linear elastic part and a plastic part which is zero before the threshold σ_s:

$$|\sigma| < \sigma_s \rightarrow \varepsilon = \varepsilon_e = \sigma/E$$
$$|\sigma| \geqslant \sigma_s \rightarrow \varepsilon = \varepsilon_e + \varepsilon_p = \sigma/E + g(\sigma).$$

Fig. 3.28. Elastic perfectly plastic solid.

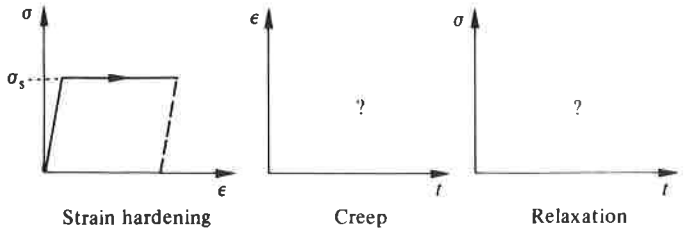

The corresponding analogical model is the generalized Saint–Venant model. Assuming that the thresholds σ_{s_i} are in increasing order and that the threshold has just been reached for the element j, its constitutive equation is the following:

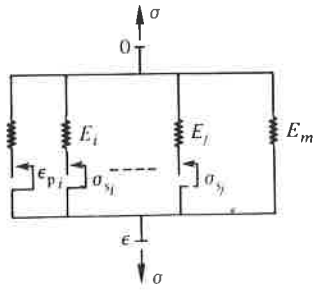

$$\sigma = \sum_{1}^{j} \sigma_{s_i} + \sum_{j+1}^{m} E_i \epsilon$$

$$\epsilon = \begin{cases} \dfrac{\sigma_{s_i}}{E_i} + \epsilon_{p_i} & \sigma_i = \sigma_{s_i} \\ \dfrac{\sigma_i}{E_i} & \sigma_i < \sigma_{s_i} \end{cases}$$

The stress–strain curve is piecewise linear, the threshold stresses are given by:

$$\sigma'_{s_j} = \sum_{1}^{j-1} \sigma_{s_i} + \frac{\sigma_{s_j}}{E_j} \sum_{j}^{m} E_i.$$

Its hardening curve after unloading from tension can be derived from its hardening curve in compression by a homothetic transformation with ratio 2 and a centre P' symmetrical to the unloading point P with respect to the origin 0 (Fig. 3.30).

Applications: metals and alloys at temperatures lower than one quarter of their absolute melting temperature (expressed in K).

3.3.6 *Viscoplastic solids*

Viscoplastic solids are those which exhibit permanent deformations after the application of loads (like plastic solids) but which continue to undergo a

Fig. 3.29. Elastoplastic hardening solid.

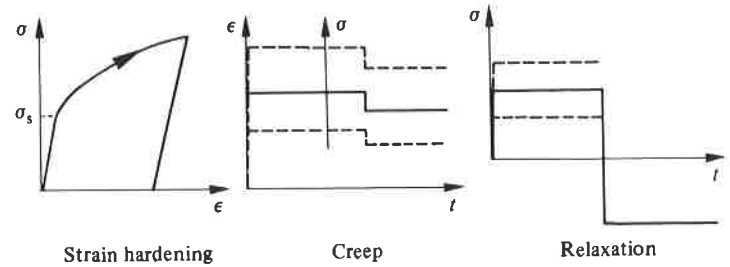

creep flow as a function of time under the influence of the applied load (equilibrium is impossible). They are studied in Chapter 6.

Perfectly viscoplastic solid (Fig. 3.31)

The rate of permanent strain (as for viscous fluids) is a function of the stress: $\sigma(\dot{\varepsilon})$.

Norton model

$$\sigma = \lambda \dot{\varepsilon}^{1/N}.$$

Fig. 3.30. Stress–strain curve for the generalized Saint–Venant model.

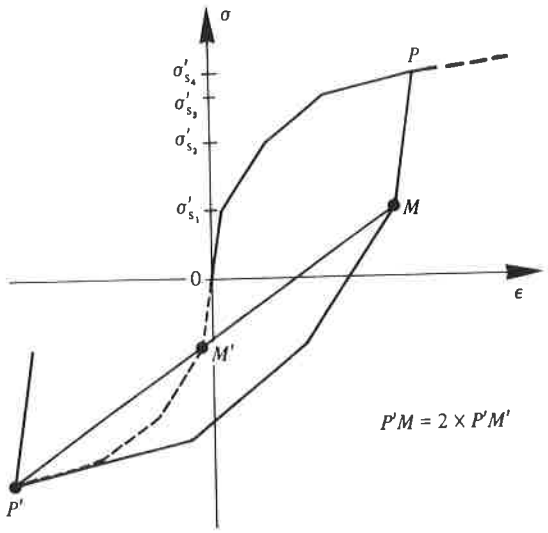

Fig. 3.31. Perfectly viscoplastic solid.

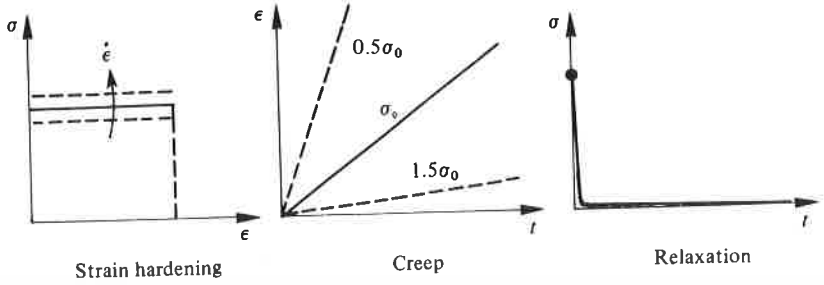

Applications: rough schematic representation of metals and alloys at temperatures higher than one third of their absolute melting point (in K).

Elastic perfectly viscoplastic solid (Fig. 3.32)

The elasticity is no longer considered negligible but the rate of plastic strain is only a function of the stress. There is no influence of hardening.

$$|\sigma| < \sigma_s \rightarrow \varepsilon = \varepsilon_e = \sigma/E$$
$$|\sigma| \geqslant \sigma_s \rightarrow \varepsilon = \varepsilon_e + \varepsilon_p \quad \dot{\varepsilon} = \dot{\sigma}/E + f(\sigma).$$

Bingham–Norton Model:

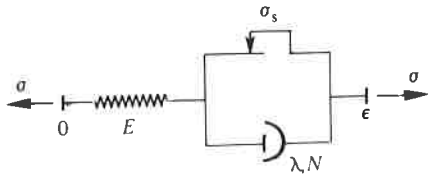

$$\sigma < \sigma_s \rightarrow \quad \sigma = E\varepsilon$$
$$\sigma \geqslant \sigma_s \rightarrow \begin{cases} \varepsilon = \varepsilon_e + \varepsilon_p \\ \sigma = E\varepsilon_e = \sigma_s + \lambda \dot{\varepsilon}_p^{\,1/N}. \end{cases}$$

Its response to a relaxation test is:

$$\varepsilon = \varepsilon_0 H(t) \rightarrow \sigma = \sigma_s + \frac{E\varepsilon_0 - \sigma_s}{\left[1 + \dfrac{(N-1)E}{\lambda^N}(E\varepsilon_0 - \sigma_s)^{N-1} t\right]^{1/(N-1)}}.$$

Elastoviscoplastic hardening solid (Fig. 3.33)

This is the most complex schematic representation because the stress depends on the plastic strain rate and on the plastic strain itself or on some

Fig. 3.32. Elastic perfectly viscoplastic solid.

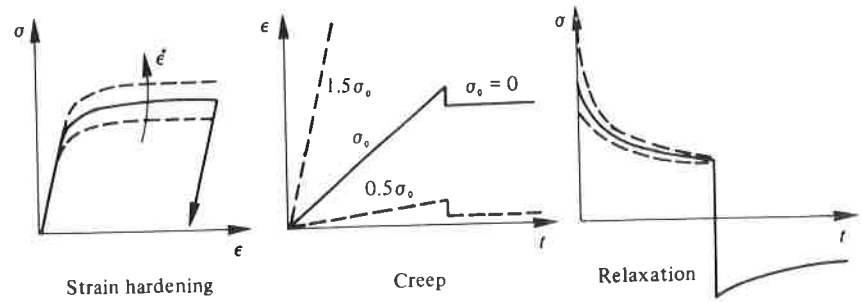

other hardening variable.

$$|\sigma| < \sigma_s \rightarrow \varepsilon = \varepsilon_e = \sigma/E$$
$$|\sigma| \geqslant \sigma_s \rightarrow \varepsilon = \varepsilon_e + \varepsilon_p$$
$$\sigma = E\varepsilon_e = f(\varepsilon_p, \dot{\varepsilon}_p).$$

Applications: metals and alloys at medium to high temperatures, wood under high loads.

3.3.7 *Characterization of work-hardening*

There are different ways of schematically representing the hardening of materials induced by deformations.

Isotropic hardening

Even though most materials exhibit a strong, hardening induced anisotropy, the isotropic hardening representation is very often used. This is because of its simplicity and because it is a good representation in the case of proportional loading, i.e. when the representative stress vector maintains a constant direction in the stress space.

In order to demonstrate the presence of this isotropy, or lack of it (i.e. anisotropy), we must examine the results of experiments conducted with different load directions: biaxial tension tests, tension (or compression) and torsion tests. The initial anisotropy is detected by tests conducted on samples taken in different directions with respect to the material. A material will be considered to justify the hypothesis of isotropic hardening if the boundary of the elastic domain is found to depend only on a scalar parameter (Fig. 3.34).

Fig. 3.33. Elastoviscoplastic solid.

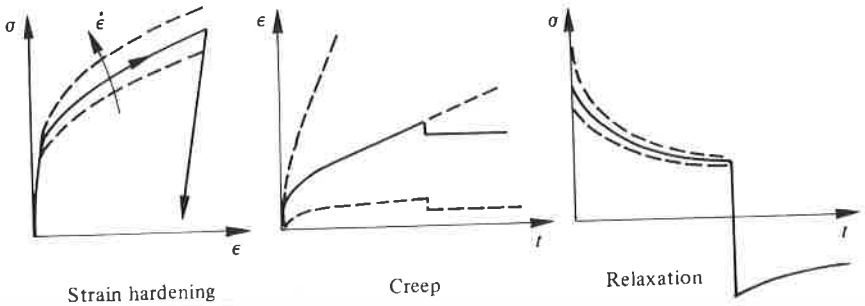

The compression curve subsequent to the initial loading in tension in a work-hardening test can be derived from the monotonic tensile curve by a homothetic transformation with ratio 1 and with centre at the point of the zero stress (point B in Fig. 3.34).

The loading curves, which represent points corresponding to the limit of elasticity in a two-dimensional stress space, of normal stress and shear stress (tension–torsion tests on thin tubes at different states of hardening), are derived from one another by homothetic transformation about the centre 0 (Fig. 3.34).

Kinematic hardening

A very useful schematic representation of anisotropic hardening is that of linear kinematic hardening in which the elastic domain retains a constant size but moves about in the stress space by translation. The 'centre of the elastic domain' (C in Fig. 3.35) represents the internal stress of the neutral state (or back stress).

The one-dimensional compression curve can be derived from the new tension curve by a homothetic transformation with ratio -1 and centre C.

In the tension–torsion test the loading curves corresponding to different hardening states can be derived from one another by translation of the vectors such as $\overrightarrow{OC}$.

Fig. 3.34. Isotropic hardening: (*a*) tension–compression test; (*b*) tension–torsion test.

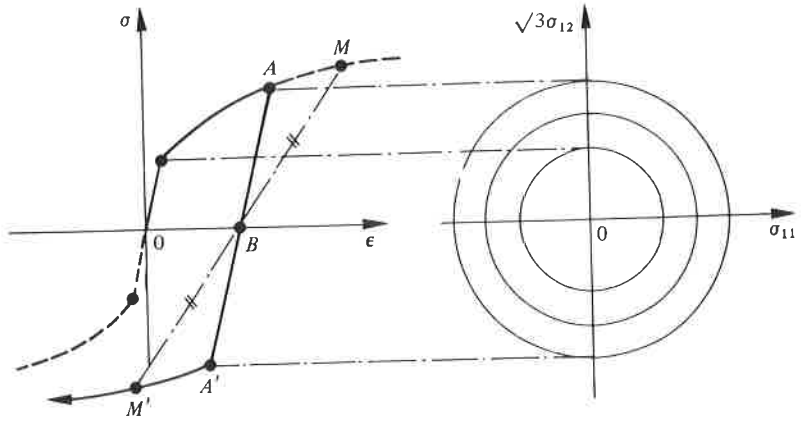

Bauschinger effect

The Bauschinger effect manifests itself when a specimen is subjected to a tension test followed by a compression test; it is often found that since the tension test was carried out first, the material has hardened in tension (increased yield stress) but has softened in compression. Fig. 3.36 shows that the yield stress in compression is lower than that if the test were carried out in compression first.

Of the two simple schematic representations mentioned above, the kinematic hardening one is closer to the real case and represents a first approximation to the Bauschinger effect.

Effect of cyclic loadings

In tension–compression cyclic loadings, most metals and alloys experience a variation in their hardening properties during the cycles. They may soften

Fig. 3.35. Kinematic hardening: (*a*) tension–compression test; (*b*) tension–torsion test.

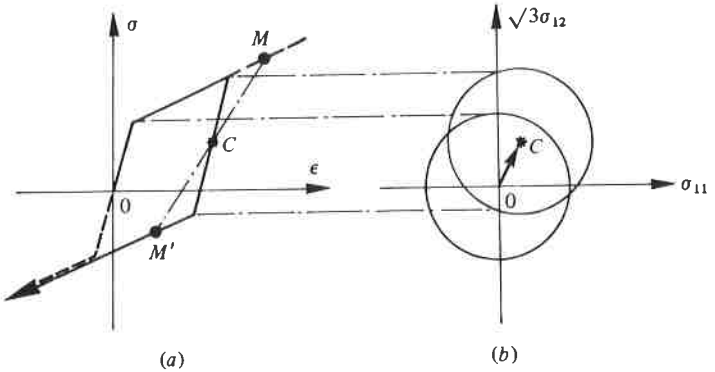

Fig. 3.36. Bauschinger effect.

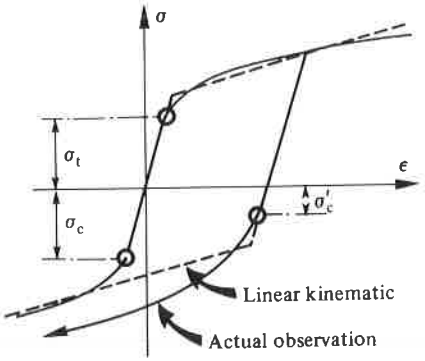

Fig. 3.37. A stress–strain cycle.

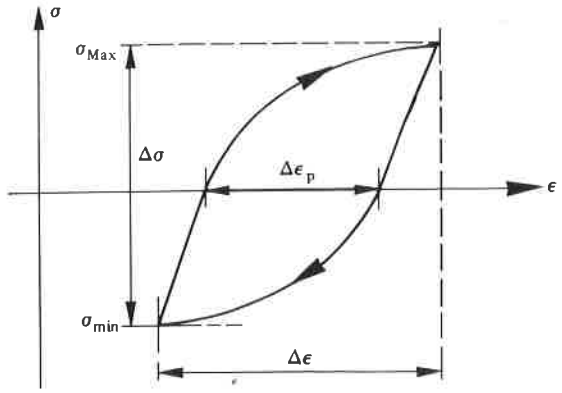

$$\bar{\sigma} = \frac{\sigma_{Max} + \sigma_{min}}{2}$$

$$\Delta\epsilon = \Delta\epsilon_e + \Delta\epsilon_p = \Delta\sigma/E + \Delta\epsilon_p$$

Fig. 3.38. Phenomenon of cyclic softening: (*a*) controlled strain; (*b*) controlled stress

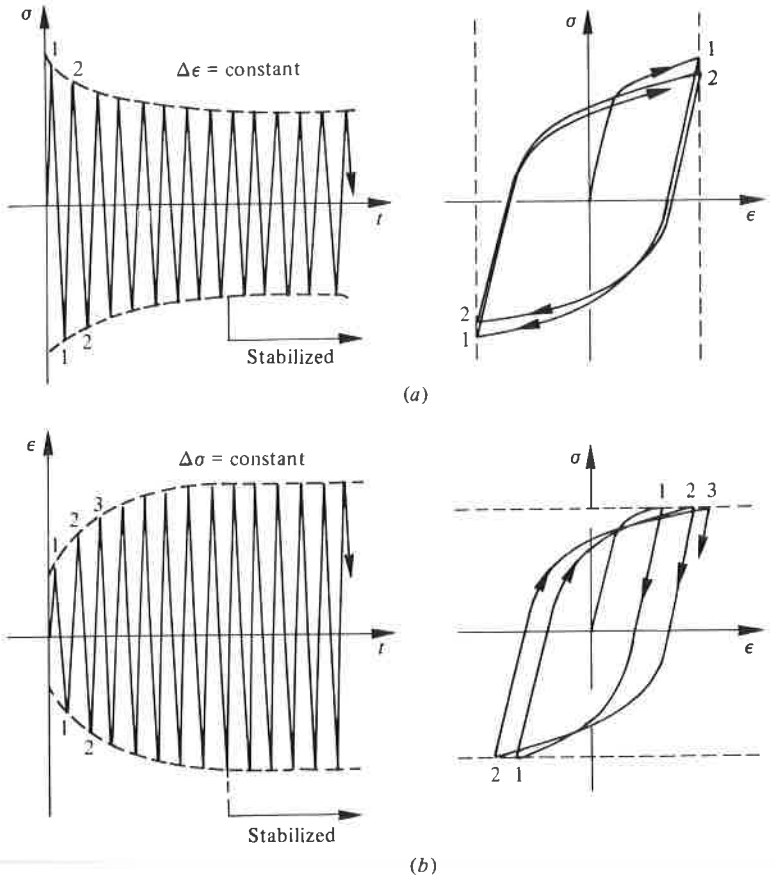

or harden depending on the material, temperature, and the initial state. The quantities generally used in describing the results of cyclic tests (with stabilized cycles) are defined in Fig. 3.37.

The softening is said to occur when the stress range $\Delta\sigma$ decreases during successive cycles under controlled strain (Fig. 3.38(*a*)), or when the strain range $\Delta\varepsilon$ increases in a stress controlled test (Fig. 3.38(*b*)). On the other hand, a cyclic hardening corresponds to a rise in the stress range $\Delta\sigma$ when strain is controlled (Fig. 3.39(*a*)) or to a fall in the strain range $\Delta\varepsilon$ when the

Fig. 3.39. Phenomenon of cyclic hardening: (*a*) controlled strain; (*b*) controlled stress.

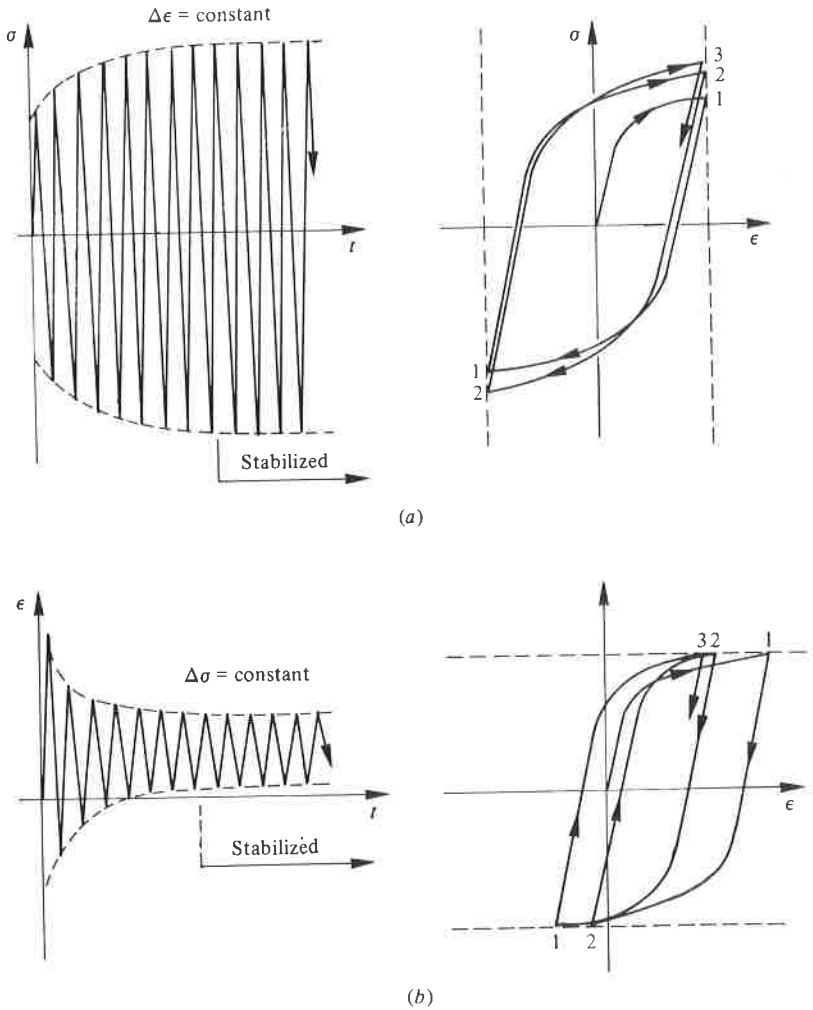

test is stress-controlled (Fig. 3.39(*b*)). When a periodic load induces a periodic response, we have stabilization in the sense that there exists a stabilized cycle (see Section 3.2.1).

If the load is not purely alternating, additional effects can occur (Fig. 3.40(*a*) and (*b*)). In nonsymmetric stress-controlled tests, either shakedown may occur or, more often, a ratchetting effect may be induced. In the case of ratchetting, there is a progressive increase in strain at each cycle, even in a stabilized regime (so that we have a periodic strain

Fig. 3.40. Phenomena of (*a*) shakedown, (*b*) ratchetting, (*c*) non-relaxation and (*d*) relaxation of the mean stress.

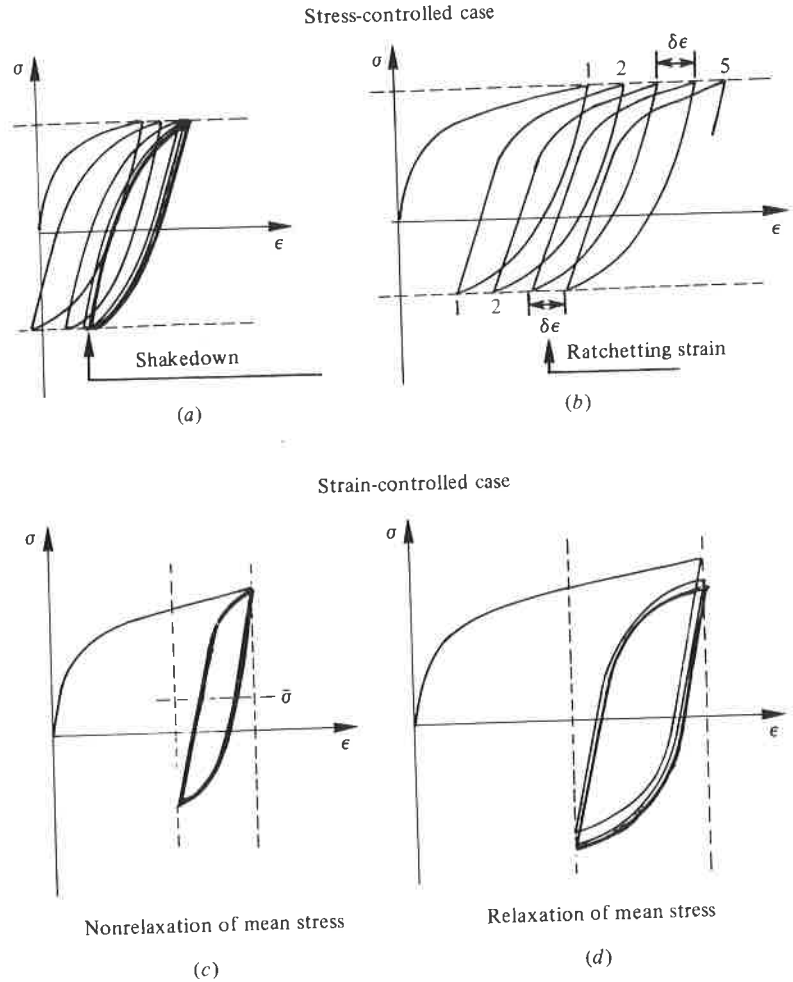

superimposed on a secular term representing progressive strain). Correspondingly, in a strain-controlled test we have the phenomena of relaxation or nonrelaxation of the mean stress (Fig. 3.40(*c*) and (*d*)).

3.3.8 *Ageing*

The materials considered in the previous sections are assumed to be stable in the sense that their characteristic properties do not change with time. The effects of ageing on a material are determined by comparing responses to characteristic tests (for example Fig. 3.41).

(*a*) The reference test is conducted before any ageing of the material (tensile test, for example).

(*b*) The same test is conducted on a specimen, initially identical, after waiting for a long or short period.

If the responses to the tests (*a*) and (*b*) are different, then ageing is said to have occurred. If the response is identical in both tests the material is stable. Materials which age include not only concrete and polymers, but also metal alloys under certain temperature conditions.

3.4 Schematic representation of fracture

Characterization of fracture remains a delicate task as it is partly founded on the physical examination of the morphology of the fractured parts and depends on the scale at which the analysis is performed: the microscopic scale of the fracture mechanisms, the macroscopic scale of volume element, and the scale of the structure. The last two lead to the modelling described in Chapters 7 and 8.

Fig. 3.41. Characteristic tests for studying the ageing of a material: (*a*) before, (*b*) after ageing, and (*c*) responses.

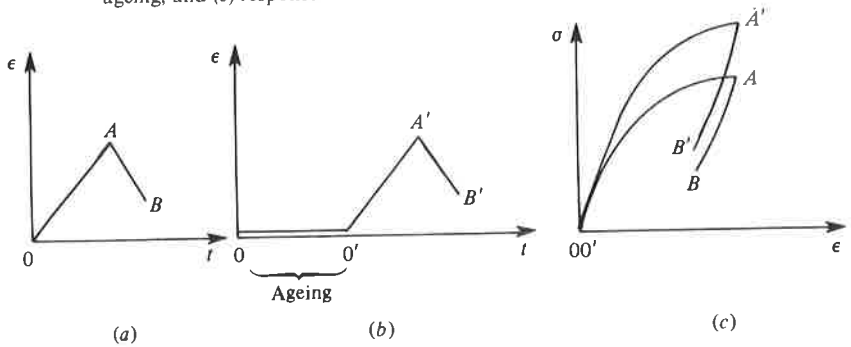

The observation of failure patterns in metals requires the preparation of samples by the use of metallographic techniques. Visual examination is limited to a resolution of the order 0.1 mm. With a binocular magnifying glass (with a maximum magnification of the order of 100 ×) it is already possible to identify the breaking zones which correspond to microbrittle fracture (shiny appearance), to fatigue fracture (dull appearance) or to a macroductile fracture (change in geometry). With an optical microscope (with a maximum magnification of the order of 1000 ×) it is possible to begin to observe the loss of cohesion associated with microbrittle fracture, the striations associated with fatigue fracture, and the cavities which lead to microductile fracture; but it is mostly with the use of the electron microscope (with magnification of 10 000 – 100 000 × and even up to 10^6 ×) that these defects can be finely analyzed so as to be able to deduce the kinematics of fracture mechanisms described in Chapter 1.

3.4.1 *Fracture by damage of a volume element*

At the level of the volume element, brittle microdecohesion and microductility induce very significant local plastic deformations. They are always present but in varying proportions, and the schematic representation depends on this proportion.

The volume element is considered as totally damaged, i.e., broken following the initiation of a macroscopic crack. In a structure, a conventional crack size of 1 mm² or a characteristic dimension of 1 mm is acceptable with respect to the crystalline or molecular nature of metals and polymers and with respect to analyses based on continuum mechanics. This dimension is of the order of 1 cm for wood and of 10 cm for concrete.

Macrobrittle damage

This is damage through decohesion experienced under monotonic loading by materials such as concrete in the absence of irreversible macroscopic strains. The only irreversible deformations which occur are due to the arrangement of the cracks constituting the damage. In a hardening test the fracture occurs without appreciable necking (Fig. 3.42(*a*)).

Ductile plastic damage

Schematically this is damage associated with large plastic strains which leads to the growth of cavities through the mechanism of microductile instability.

The accumulated plastic strain is more than $(10–50) \times 10^{-2}$.
The hardening curve possesses a large necking phase (Fig. 3.42(*b*)).

Brittle viscoplastic damage

This is the damage which occurs in conjunction with creep strain. Therefore it is concerned with metals at moderate and high temperatures at which the decohesion of microbrittle fracture at grain boundaries is dominant.

Fig. 3.42. (*a*) Hardening curve of a brittle material. (*b*) Hardening curve of a ductile material.

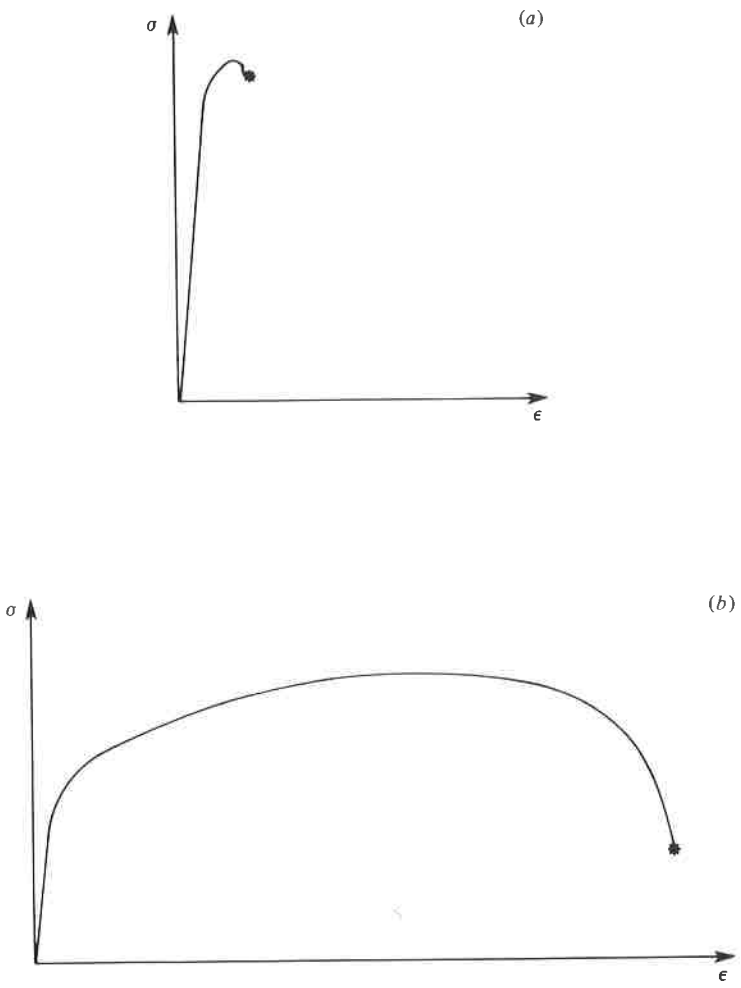

Irreversible deformations can be significant but they have no direct influence on the mechanism of decohesion. It is essentially a function of time. As the two mechanisms of decohesion and deformation are present simultaneously, this type of damage cannot be characterized by global tests. It can be detected only through a micrographic study of the fractured surfaces. An example is given in Fig. 1.19.

Fatigue damage

Under the action of repeated loads, which may or may not be periodic, microbrittle fractures occur in a discontinuous fashion with respect to time. They are often intracrystalline and appear as striations on the fractured surface. An example is given in Fig. 1.21. This damage occurs in the small strain regime and is essentially a function of the number of load cycles.

3.4.2 *Fracture by crack propagation in a structure*

When a crack is initiated in a structure (1 mm, 1 cm, 10 cm) then under the action of the load, it may grow and cause the fracture of that structure, i.e., breaking into several pieces. Here again, different mechanisms can occur, depending on the material and the type of load.

Crack propagation by brittle fracture

In this type of fracture, crack propagation results from an instability phenomenon. It spreads with great speed without appreciable plastic deformations. The only energies which come into play in creating the surface discontinuity of the crack are the stored elastic energy and the fracture energy. The graph of force versus length or area of the crack is like that shown in Fig. 3.43(*a*).

Crack propagation by ductile fracture

In this type of fracture, the crack growth is stable. It propagates with a speed which is a function of the rate of loading of the structure. In the energy balance equation, the energy dissipated in plastic deformation in the vicinity of the crack-tip must be taken into consideration. The corresponding graph is like that shown in Fig. 3.43(*b*).

Creep crack growth

In metals at high temperature, the crack can grow under a constant load at a speed which depends on the level of the load.

Fatigue crack growth

By the same mechanism as for the volume element, periodic or nonperiodic repeated loads generate a discontinuous propagation of the crack for which the number of cycles is the appropriate kinematic variable. Striations can be observed on the crack surface.

Fig. 3.43. Curve of force versus crack area: (*a*) brittle fracture, (*b*) ductile fracture.

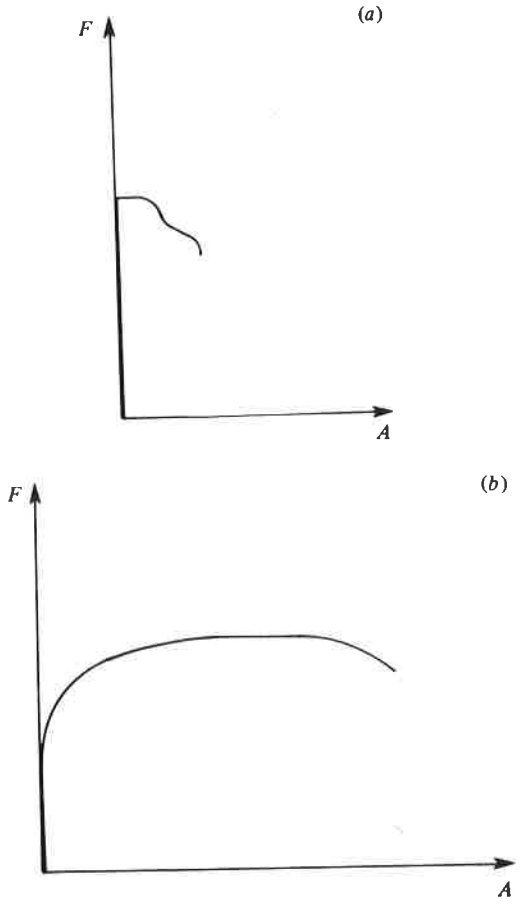

3.5 Schematic representation of friction

In problems related to forming, it becomes necessary to model frictional forces at the points of contact between the deformed material and the tool (as, for example, in the extrusion process). The interactions between the surfaces are dependent upon the roughness of the surfaces in contact as this reduces the area of real contact to a fraction of its apparent value. As a consequence, any normal force induces local stresses beyond the elastic limit.

3.5.1 *Coulomb model*

This model is derived from the theory of friction by adhesion. The coefficient of friction f is defined as the ratio of the tangential force to the normal applied force. The tangential force is expressed as the product of the real area of contact and the fracture shear stress τ_R of the less resistant of the two materials. Assuming that the normal force can be expressed by the product of real contact area and the Brinel hardness H of the materials, it follows that the coefficient of friction is: $f = \tau_R/H$ which is a quantity characteristic of the two materials in contact.

The Coulomb model expresses the shear stress σ_{12} opposing the relative translation of the two materials subjected to a normal contact stress σ_{11} in the following form:

- $\sigma_{12} = f\sigma_{11}$ if $f\sigma_{11} < \tau_R$,
- $\sigma_{12} = \tau_R$ if $f\sigma_{11} \geqslant \tau_R$.

Table 3.2 gives values of f for some materials.

3.5.2 *Boundary layer model*

A thin layer of oxides or of lubricants providing perfect adhesion between the two solids is often formed at an interface. Assuming that the relative movement between the two bodies can only take place through the shear of this layer by a shear stress equal to a fraction $\bar{m}$ of the fracture shear stress or the plastic yield stress in shear of the less resistant material, we have:

- $\sigma_{12} = \bar{m}\tau_R$

where $\bar{m}$ is the coefficient of friction of the boundary layer $0 \leqslant \bar{m} \leqslant 1$, $\bar{m} = 0$ characterizes contact without friction and $\bar{m} = 1$ characterizes the 'sticking'

Table 3.2. *Approximate values of coefficients of friction*

Metal	Temperature °C	Lubrication	f	$\bar{m}$
Mild steel	20	Dry	0.25	0.5
Mild steel	950	Dry	0.45	0.3–1
Mild steel	20	Oil	0.03	0.05
Steel	20	Soaps	0.05	0.07
Aluminium	20	Oil	0.05	0.15
Copper	20	Dry	0.1	0.9
Copper	850	Graphite	0.25	0.2

contact of materials at high temperatures. Table 3.2 gives several characteristic values of $\bar{m}$.

Bibliography

Persoz B. *Introduction à l'étude de la rhéologie*. Dunod, Paris (1960).
Malvern L. E. *Introduction to the mechanics of a continuous medium*. Prentice Hall New Jersey (1969).
Mandel J. *Propriétés mécaniques des matériaux*. Eyrolles, Paris (1978).
Lieurade H. P. *La pratique des essais de fatigue*. P.Y.C. Edition, Paris (1982).
Broyden C. G., Fletcher R., Murray W., Powel M. J. D. & Swann W. M. *Numerical methods for unconstrained optimization*. Murray Ed. (1972).
Loveday M. S., Day M. F., Dyson B. F. *Measurement of high temperature mechanical properties of materials*. National Physical Laboratory. Her Majesty's Stationery Office, London (1982).
ASTM. *Metals Handbook*: Vols. 1–12. American Society for Metals, Philadelphia.

4

LINEAR ELASTICITY, THERMOELASTICITY AND VISCOELASTICITY

Une loi est un modèle qui n'est plus (et pas encore!) contesté.

Hooke (1676), Young (1807), Cauchy (1822) and Timoshenko (1934) have said almost everything about the linear-elastic behaviour of materials. In this field, we will therefore limit ourselves to giving a summary in the form of formulae. However, we will deal with anisotropic elasticity, which is so important for composite materials, and the identification of the coefficients. The term elasticity is taken here to mean the reversible deformations mentioned in Chapter 3. Neither thermal dissipation (thermoelasticity) nor mechanical dissipation (viscoelasticity) is excluded.

Thermoelasticity introduces several additional coefficients into the constitutive law including the dilatation coefficient, and permits the treatment of problems involving temperature variations, such as thermal stress analysis problems.

The theory of viscoelasticity was developed considerably with rheology during the 1960s. We will restrict ourselves in this chapter to linear viscoelasticity which is sufficient to deal with the mechanical behaviour of certain polymers.

These theories are continuum theories; the inhomogeneities are assumed to be small enough with respect to the size of the volume element that the results of experiments conducted on the latter are really the characteristics of average macroscopic behaviour. This is also true for composite materials and concrete whose behaviour can be more accurately described by homogenization techniques.

4.1 Elasticity

4.1.1 *Domain of validity and use*

All solid materials possess a domain in the stress space within which a load variation results only in a variation of elastic strains. As discussed in